

**MEASURING UNIFORMITY IN KRAFT DIGESTERS  
USING FLOW-FOLLOWING SENSORS**

by

**Elham Albadvi**

**BEng (Hons), The University of Manchester, 2008**

**A THESIS SUBMITTED IN PARTIAL FULFILMENT OF  
THE REQUIREMENTS FOR THE DEGREE OF**

**MASTER OF APPLIED SCIENCE**

in

**The Faculty of Graduate Studies**

**(Chemical and Biological Engineering)**

**THE UNIVERSITY OF BRITISH COLUMBIA**

**(Vancouver)**

**October 2010**

**© Elham Albadvi, 2010**

## **Abstract**

Measurements of pulp variability and temperature distributions within kraft digesters have been the subject of intense interest for many years. An extensive survey carried out on the previous approaches to measure digester variability has shown that data directly taken from within the digester, during the kraft cook is scarce. Moreover, the increased size of modern digesters is believed to reduce the flow uniformity within them, increasing the risk of pulp variability and highlighting the need to collect data from within the digesters themselves. This has motivated the development of a new method for measuring digester variability: the “SmartChip”. This device is a flow-following sensor package that measures and records the temperature directly within the digester during the kraft cook.

This research proposes a theoretical model to describe the heat transfer mechanisms occurring within the digester and then uses the data captured by the SmartChip to measure the digester variability. Preliminary test trials were conducted to ensure that the SmartChip could withstand the harsh environment of the kraft cook. Subsequently, multiple SmartChips were deployed in a single cook to provide insight on the temperature variability and heat transfer mechanisms occurring within the digester and these experimental results were then be compared with the predictions of the proposed model. Moreover, by taking pulp samples in the vicinity of the SmartChip sensors, the relation between nonuniformity and temperature gradients is established.

The SmartChips have been tested in two laboratory batch digesters and as expected, temperature was already well-controlled within them and little variability was observed in these small-scale devices. Moreover, a good agreement is found between the model predictions and the experimental results and the model is experimentally validated, showing that the heat transfer through the digester contents is by pure advection with almost negligible thermal energy required for the heating of wood chips. These findings further suggest that the SmartChip works well under the harsh conditions of the kraft cook and future work is warranted to develop the instrument for its use at the industrial scale, where the temperature fluctuations along the digesters are more noticeable.

## Preface

Modified versions of Chapters 5 to 7 were published in two manuscripts in the Journal *Pulp and Paper Canada*: **(1)** T. C. M. Graham, E. Liu, A. R. Mohammadi, N. Sadeghi, E. Albadvi, S. Mirabbasi, M. Chiao, J. Madden and C. P. J. Bennington, “Development of a Flow-Following Sensor Package for Application in Chemical Pulp Digesters” **(2)** E. Albadvi, T. C. M. Graham, E. Liu, M. Alaqqad, C. P. J. Bennington, R. J. Kerekes, M. Martinez, and S. Mirabbasi, “Measuring Uniformity in Kraft Digesters using Flow-Following Sensors.”

With directions from my supervisors: Dr. Bennington, Dr. Martinez and Dr. Mirabbasi, my contribution was testing the SmartChips in the digesters including development of the experimental plan, collection and analysis of data and discussion of results. Tim Graham contributed significantly through his help in performing the experiments and analysis of the findings. Edward Liu and Tim Graham also contributed by the calibration of the SmartChip, presented in Appendix C and Mohammad Alaqqad contributed by helping with the digester kraft cooks in the 20L batch digester. For the first manuscript mentioned above, my contribution was as co-author, with Tim Graham being the first author. For the second manuscript mentioned above, I was the first author and wrote the manuscript with revisions, suggestions and discussions of the findings from Dr. Graham, Dr. Martinez, Dr. Mirabbasi, Dr. Kerekes and Dr. Bennington.

Another manuscript: **(3)** E. Albadvi, T. C. M. Graham, E. Liu, C. P. J. Bennington, R. J. Kerekes, M. Martinez, and S. Mirabbasi, “Application of the SmartChip to Measure Uniformity and Heat Transfer in Kraft Digesters” is being prepared for publication based on the findings in Chapter 4 and Chapter 7. With the direction and supervision of Dr. Martinez, I have developed a theoretical model describing the heat transfer mechanisms occurring within the digester and then validated the model with experimental data. Tim Graham contributed significantly through his help in performing the experiments and analysis of the results. I am the first author of this manuscript, with revisions, suggestions and discussions of the findings from Dr. Graham, Dr. Martinez, Dr. Mirabbasi, Dr. Kerekes and Dr. Bennington.

# Table of Contents

<b>Abstract .....</b>	<b>ii</b>
<b>Preface .....</b>	<b>iii</b>
<b>Table of Contents.....</b>	<b>iv</b>
<b>List of Tables.....</b>	<b>vi</b>
<b>List of Figures .....</b>	<b>vii</b>
<b>Nomenclature .....</b>	<b>x</b>
<b>Acknowledgements .....</b>	<b>xii</b>
<b>1. Introduction .....</b>	<b>1</b>
<b>1.1 Thesis Objectives .....</b>	<b>2</b>
<b>1.2 Thesis Organization.....</b>	<b>2</b>
<b>2. Background .....</b>	<b>3</b>
<b>2.1 Overview of the Pulping Industry .....</b>	<b>3</b>
<b>2.2 Delignification Uniformity .....</b>	<b>4</b>
2.2.1 Effects of Kraft Pulp Variability.....	5
2.2.2 Sources of Kraft Pulp Variability .....	7
<b>2.3 Industrial Operations .....</b>	<b>9</b>
2.3.1 Batch Digesters.....	9
2.3.2 Continuous Digesters.....	11
<b>3. Review of Literature.....</b>	<b>14</b>
<b>3.1 Previous Works on Measuring Digester Variability .....</b>	<b>14</b>
3.1.1 Batch Digesters.....	14
3.1.2 Continuous Digesters.....	18
<b>4 Modeling Heat Transfer in Kraft Digesters .....</b>	<b>21</b>
<b>4.1 The Significance of Temperature in Pulping Kinetics .....</b>	<b>21</b>
<b>4.2 Model Development .....</b>	<b>22</b>
<b>4.3 Thermo-physical Properties of Wood.....</b>	<b>26</b>
4.3.1 Density.....	26
4.3.2 Specific Heat Capacity .....	26
4.3.3 Thermal Conductivity.....	27
<b>4.4 Model Solution .....</b>	<b>27</b>

<b>5</b>	<b>The “SmartChip” .....</b>	<b>29</b>
<b>5.1</b>	<b>The “SmartChip” – What is it? .....</b>	<b>29</b>
<b>5.2</b>	<b>The “SmartChip” Components.....</b>	<b>31</b>
<b>6</b>	<b>Experimental Methods .....</b>	<b>34</b>
<b>6.1</b>	<b>Single SmartChip Testing .....</b>	<b>34</b>
<b>6.2</b>	<b>Multiple SmartChips in a Single Cook.....</b>	<b>35</b>
6.2.1	Multiple SmartChips in 5L M/K Batch Digester.....	35
6.2.2	Multiple SmartChips in 20L Batch Digester .....	35
<b>7</b>	<b>Results and Discussions.....</b>	<b>37</b>
<b>7.1</b>	<b>Single SmartChip Testing .....</b>	<b>37</b>
<b>7.2</b>	<b>SmartChip Trials in 5L M/K Batch Digester .....</b>	<b>41</b>
7.2.1	Experimental Results .....	42
7.2.2	Model Validation .....	46
<b>7.3</b>	<b>SmartChip Trials in 20L Batch Digester.....</b>	<b>49</b>
<b>8</b>	<b>Closing Remarks.....</b>	<b>52</b>
<b>8.1</b>	<b>Summary and Conclusions .....</b>	<b>52</b>
<b>8.2</b>	<b>Recommendations and Future Work.....</b>	<b>53</b>
	<b>References.....</b>	<b>55</b>
	<b>Appendices .....</b>	<b>60</b>
	<b>Appendix A: Pulping Chemical Preparation .....</b>	<b>60</b>
	<b>Appendix B: Kappa Number Determination .....</b>	<b>62</b>
	<b>Appendix C: Calibration.....</b>	<b>64</b>
	Electronics Calibration .....	65
	Sensor Calibration .....	68
	Time Calibration.....	71

## List of Tables

<b>Table 1:</b> Specifications and kappa test results for five kraft cooks conducted in a 5L M/K laboratory batch digester with a single SmartChip positioned in the centre, under the cook conditions specified in section 6.1, but varying cook temperature and time-at-cook temperature.....	39
---	----

## List of Figures

<b>Figure 1:</b> Schematic of a Batch Digester with indirect steam heating.....	10
<b>Figure 2:</b> Schematic of an EMCC System.....	12
<b>Figure 3:</b> Variation of kappa number as a function of location within an industrial batch digester based on the “triple-hanging-basket” technique reported by MacLeod [16]......	15
<b>Figure 4:</b> Variation of kappa number at the digester blow line, as a function of time in an industrial batch digester as reported by Lee and Bennington [29]. .....	17
<b>Figure 5:</b> Kappa variation in an Extended Modified Continuous Cooking System with chemical kappa testing on 72 pulp samples taken at the digester blow line at 30s intervals over a half hour period.....	19
<b>Figure 6:</b> Histogram of the kappa distribution in the EMCC system based on the results from Figure 5.....	19
<b>Figure 7:</b> Schematic of the 5L M/K batch digester system, showing the dimensions and geometry of the digester for modeling the heat transfer processes occurring within it.....	22
<b>Figure 8:</b> A photograph of two SmartChips – one to show the SmartChip electronics and another to show the alignment of the sensors on the outside. The SmartChip package has a diameter of approximately 7.5 cm. ....	30
<b>Figure 9 :</b> Block Diagram of SmartChip prototype components and the communication between them.....	32
<b>Figure 10:</b> Time/temperature data measured (1) by a single SmartChip (with $10 \times 6 \text{ cm}^2$ PTFE package) placed in the centre of the digester and (2) by the sensor at the liquor circulation loop of the digester, during a kraft cook. The cook took place in a 5L M/K laboratory batch digester, with a cook time of 165 minutes at 170°C. An inset figure is provided for better illustration of the temperature variability and lag.....	37
<b>Figure 11:</b> Correlation between H-factor and Kappa number for the digester cooks given in Table 1 .....	39

**Figure 12:** Time/temperature data measured (1) by a single SmartChip (with  $7.5 \times 4 \text{ cm}^2$  PEEK package and its two sensors I-RTD and E-RTD ), placed in the centre of the digester and (2) by the digester temperature sensor at the outlet, during a kraft cook. The 5L M/K laboratory batch digester was employed; with the cook time of 165 minutes at 170°C. An inset figure for the time-at-cook temperature is provided for better illustration of the temperature variability..... 41

**Figure 13:** Time/temperature data measured by two SmartChips, SC001 placed at the top and SC002 placed at the bottom – approximately 20 cm apart. Wood chips were cooked in a 5L M/K laboratory batch digester, with the cook time of 165 minutes at 170°C. Inset figures are provided for better illustration of temperature variability and lag..... 43

**Figure 14:** Magnification of the initial temperature oscillation for both SmartChips (SC001 placed at the top and SC002 placed at the bottom) once the cook just reaches the maximum temperature. This is to show the temperature lag and decrease in amplitude, moving down the digester length..... 44

**Figure 15:** The difference in the time at which the E-RTD sensor on each SmartChip reaches the peak temperature, i.e., the y-axis is  $[(t_{\text{PEAK,SC002}}) - (t_{\text{PEAK,SC001}})]$  and the x-axis is the peak number during the time-at-cook temperature– there are 34 peaks in total during the time-at-cook temperature for this case. .... 45

**Figure 16:** Time/temperature data measured by the SmartChips SC001 and SC002 in the 20L batch digester during a kraft cook. For the first trial (left figure), the time-at-cook temperature was 51 minutes, SC001 at the bottom and SC002 at the top of the digester. In the second trial (right figure), the time-at-cook temperature was 106 minutes, with the SmartChip positions inverted. An inset figure is given to better illustrate the temperature variability and lag. .... 50

**Figure 17:** Kappa test results from pulp samples taken from the top, bottom and middle of the digester, for three cooks in the 20L batch digester. For each trial, the wood chips are cooked for varying time-at-cook temperatures resulting in varying target H-factors. .... 51

**Figure C1:** Schematics of the Wheatstone Bridge Temperature Sensor. .... 64

**Figure C2:** Typical arrangement of sensor and electronics..... 65

**Figure C3:** (a) Measuring the uncalibrated electronics error for both sensor ports (I-RTD and E-RTD) on SC001 over the SmartChip temperature range when the SmartChip is heated up to 180°C and then allowed to cool back down to 25°C in 2 hours (b) Calibrated electronics error for both sensor ports (I-RTD and E-RTD) on SC001 over the SmartChip temperature range for the same run. .... 67

**Figure C4:** Calibrated electronics error for both sensor ports (I-RTD and E-RTD) on SC001 over the SmartChip temperature range when the SmartChip is heated up to 180°C and then allowed to cool back down to 25°C in 2 hours – the calibration constant for the previous run are applied to a subsequent run to verify that calibration holds. .... 68

**Figure C5:** Time-temperature data logged by the sensor ports (I-RTD and E-RTD) on SC001 when placed in an oven that was heated and allowed to settle at three set points. .... 69

**Figure C6:** Fitting the Callendar–Van Dusen to the actual temperature readings taken by each sensor port (I-RTD and E-RTD) on SC001 so as to readjust the A and B constants in this equation. .... 70

**Figure C7:** Calibrated temperature readings for both sensor ports (I-RTD and E-RTD) on SC001 when placed in an oven that was heated and allowed to settle at three set points - the calibration constant for the previous run are applied to a subsequent run to verify that calibration holds. .... 71

**Figure C8:** The variation in the sampling interval with temperature while the SmartChip was cooled down from 180°C. .... 72

**Figure C9:** Comparison of the (a) uncalibrated and (b) calibrated interval error over the SmartChip temperature range of 40°C to 180°C. .... 72

## Nomenclature

$a$	Amount of thiosulphate consumed by the test specimen, mL
$b$	Amount of thiosulphate consumed in the blank determination, mL
$c_p$	Specific heat capacity, J/kg.K
$E_a$	Activation energy, kJ/mol
$EA$	Effective alkali content, % on wood
$f$	Factor for correction to a 50% permanganate consumption
$f_{temp}$	Factor for temperature correction
$G_b$	Specific gravity based on green volume
$G_m$	Specific gravity based on volume
$H$	H-factor
$h$	Interphasial heat transfer coefficient, W/m <sup>2</sup> K
$K$	Kappa number of pulp
$k$	Thermal Conductivity, W/kg.m
$L$	Vertical length of digester, m
$M$	Moisture content in wood, %
$N$	Normality of the thiosulphate
$p$	Amount of 0.1N permanganate actually consumed by the test specimen, mL
$q''$	Internal heat source per unit volume, J/m <sup>3</sup>
$R$	Ideal gas constant, kJ/mol.K
$T$	Temperature, K
$t$	Time, s
$T^*$	Dimensionless temperature
$t^*$	Dimensionless time
$t_a$	Advective time scale, s
$T_a$	Ambient temperature, K
$T_p$	Predefined temperature schedule, K
$T_{max}$	Maximum cook temperature, K
$T_r$	Actual reaction temperature, °C

$v$	Velocity of the fluid phase, m/s
$x$	Axial distance along the digester, m
$x^*$	Dimensionless distance
$y$	Sulphidity
$z$	EA charge
$\alpha, \beta, n$	Constants dependant on wood species for kappa determination
$\epsilon$	Porosity
$\rho$	Density, kg/m <sup>3</sup>

## **Acknowledgements**

I owe everlasting gratefulness to many people who pleasantly involved themselves in helping me undertake this thesis.

First and foremost I owe my deepest appreciation to my supervisors, Dr. Mark Martinez, Dr. Shahriar Mirabbasi and Dr. Chad Bennington, for providing ongoing guidance, encouragement and support during my research. Sadly, Dr. Bennington passed away on February 14, 2010 during the course of my study, but without his inspiration and motivation, this work would never have been possible. I would also like to thank my committee members, Dr. Richard Kerekes and Dr. James Olson, for the review of this dissertation and subsequent examination. I am also deeply indebted to Dr. Tim Graham whose help, suggestions and ideas contributed significantly to my research work.

The support of this research from NSERC and the industrial partners, FPInovations, Howe Sound Pulp and Paper, and SST Wireless is gratefully acknowledged. I am particularly thankful to FPInnovations VanLab who provided the 20L laboratory batch digester used to collect many of the results presented in this research.

Finally, I thank my family, particularly my father Amir, my mother Shahla and my brother, Parham, who have always encouraged and believed in me and have been my key motivation during the course of my study. My thanks are also extended to all my friends for their support, patience and understanding.

# 1. Introduction

The digester is the initial stage in the conversion of wood chips to pulp and plays a critical role in shaping the kraft pulp qualities. The key objective in the optimization of digester performance is improving the uniformity of pulp produced. In an ideal situation, each fibre should receive equal treatment chemically, resulting in all processed fibres having equal residual lignin contents and producing uniform pulp. However, in practise, this may not be the case due to anomalies within the pulping environment.

Measuring variability within kraft digesters has been the subject of intense investigation for the past half-century. Many approaches have been taken to determine the extent of delignification diversity within digesters, including kappa number variability measured as a function of location in the digester during pulp discharge and temperature variability measured at the digester walls. However, data taken directly from within the digester, during the cook, are scarce in the analysis of variability thus far. In fact, the literature reports only one previous attempt to deploy a flow-following device through a continuous kraft digester. This was in 1961, by Hamilton [1], who traced the passage of six radioactively-tagged chips and confirmed the plug flow motion of the wood chips through the digester. Adding to this, the growing demand for increased pulp production capability has led to an increase in the size of modern digesters, with each new mill being built larger than the last. While this has lowered the cost per tonne of pulp by taking advantage of the scales of economy, it has increased the risk of pulp variability within the digester [2].

Previous works have shown that nonuniform pulp from the digester has a significant impact on the economic and environmental performance of the pulp and paper industry. In Canada alone, a 1% improvement in digester operation efficiency through uniform pulp production would be worth about \$80 million/year [3]. Thus, a better understanding of heterogeneity in kraft digesters would lead to improved digester performance and better quality of pulp produced. This has highlighted the need to collect data from within the digesters themselves, motivating the development of the SmartChip and leading to the objectives of this thesis.

## **1.1 Thesis Objectives**

This research introduces a new method of measuring digester variability: the “SmartChip”. This device is a flow-following sensor package that experiences the same conditions as the wood chips and measures the temperature directly inside the digester throughout the cook. Multiple SmartChips deployed in a single cook would then determine the temperature distribution inside the digester.

The primary objective of this research is the use of the SmartChips to attain insight on the temperature variability and heat transfer mechanisms occurring within the digester. A secondary objective is the development of a theoretical model describing the heat transfer processes occurring within the digester and then verifying the theoretical predictions with experimental data from the SmartChip results.

## **1.2 Thesis Organization**

The structure of this thesis is divided into eight chapters. The first two chapters introduce the background for this study, including an overview of the kraft pulping process, the causes and effects of variability within digesters as well as the thesis objectives. The literature review presented in Chapter 3 covers the various past approaches to measure variability within batch and continuous digester systems. The theoretical work is presented in Chapter 4, which includes the development of a mathematical model to describe the heat transfer mechanisms occurring within the digester. Chapter 5 introduces a new method for measuring digester variability: the SmartChip. This chapter gives some insight on the SmartChip development and its building blocks. Chapter 6 describes the experimental methods for the SmartChip digester trials and Chapter 7 presents and discusses the results from the experiments. This chapter also validates the model presented in Chapter 4 by comparing the theoretical predictions with experimental results from the SmartChips. Finally, Chapter 8 provides concluding remarks of this research work as well as looking into the areas of future study.

## **2. Background**

### **2.1 Overview of the Pulping Industry**

Wood in its natural form goes through a succession of industrial processes to be converted into fibrous raw material known as pulp, which is primarily used for the manufacture of paper and paperboard products. Canada occupies a prominent position in the international pulp market, accounting for 21% of the global market pulp supplies in 2005 [4]. The pulp and paper industry is the largest of Canada's manufacturing industries, playing a significant role in the country's economy, particularly in British Columbia. In BC alone, there are 23 operating facilities that manufacture products ranging from market pulp to high value magazines. The 23 facilities together, have an annual capacity of 8.4 million tonnes with a sales value totalling to almost seven billion [5].

With the diverse range of paper products available, a variety of pulp production processes exist, ranging from chemical, to chemi-mechanical to mechanical – each producing pulps with unique attributes. Chemical pulping relies primarily on chemical reactants and high temperatures, whereas mechanical pulping relies on mechanical treatment by abrasive refining and grinding [6]. Among these techniques, chemical pulps have dominated the market for wood pulps accounting for 93% of the world's pulp deliveries in 2008, and it is likely that it will remain so in the near future [4].

The kraft process accounts for the majority of the worldwide chemical pulp production, due to its ability to produce higher yields and superior fibre characteristics in comparison to other chemical pulping processes. The process route starts in the digester, where the wood chips are subjected to cooking liquor and elevated temperatures, separating the fibres from the lignin. The cooking liquor, a solution of mainly sodium sulphide and sodium hydroxide, chemically dissolves the lignin that holds the wood fibres together in the wood matrix to produce pulp. Digesters routinely achieve more than 90% delignification of the wood, hence playing a critical role in shaping the pulp and paper qualities [7]. The small amounts of residual fibres are then progressively removed through a series of increasingly selective delignification and bleaching/brightening steps, which will render the fibres white and give the pulp the required characteristics for the succeeding papermaking operations. Despite being more selective than the cooking process, the succeeding

pulping stages are significantly more expensive and more environmentally aggressive. Hence, the goal in the pulp mills nowadays is to promote as much delignification as possible in the digester [8].

Canada and the United States are known to be the world's largest market pulp suppliers. However by 2006, Brazil achieved higher competitiveness in the international market for wood pulp than these countries with the more long-standing forestry traditions. The boom in the Brazilian pulp and paper industry rooted from the country's favourable climate conditions, enabling fast and high quality growth cycles and low production costs [9]. Hence, for North America to assure its continued capability and attain a competitive edge over this new competition, the industry had to be as efficient and environmentally sound as possible. A key factor to achieving this objective would be the production of uniform pulp in the digester.

## **2.2 Delignification Uniformity**

The uniformity of pulping and ways to improve it have recently attracted a great deal of attention, becoming a key issue in optimizing the performance of kraft pulp digesters. Delignification uniformity refers to the ability of the process to provide the same reaction conditions in all parts of the digester vessel, such that each fibre receives equal treatment chemically, resulting in all processed fibres having equal residual lignin contents. However, this may not typically be the case due to anomalies within the pulping environment. Consider wood chips being delignified within the digester, experiencing a spectrum of chemical reactions. It is unlikely that a single chip will experience the exact same reaction conditions throughout the interior space of the digester during its travel, and it is even more unlikely that all the chips within the digester would experience identical thermal and chemical history all through their passage along the digester [10].

Surveys have shown that in 2008, there was an increasing trend in the worldwide pulp consumption by 1.1% since the previous year and by more than 40% since the last decade [11]. This increase in the worldwide kraft pulp demand has led to the continued expansion in the size of the kraft pulp digesters resulting in reduced flow uniformity within them [2]. This section details an investigation into the impact of nonuniformity on the economic and environmental performance of the pulping industry, as well as the potential sources of digester variability.

### 2.2.1 Effects of Kraft Pulp Variability

Previous studies have shown that nonuniform pulp from the digester is weaker, harder to bleach and may lead to complications in the downstream papermaking operations [12-18]. Tichy and Procter [12] conducted a study on two normally distributed nonuniform pulps, with an average kappa number of 35 but different kappa distributions (kappa standard deviations of 17 and 22), comparing them with respect to bleaching chemical demand based on a CEHDED bleaching sequence. The results showed that the more nonuniform pulp required higher bleach plant loadings, 17% higher chlorination charge and 12% higher hydroxide charge, in order to achieve the target brightness endpoint. The chemicals employed in the bleaching stage account for approximately 10% of the total production cost for market pulps, with the cost to bleach a softwood pulp being ~\$1.30 Cdn per tonne of bleached pulp for each additional kappa number [13,14]. As the nonuniformity of the cook increases, the average kappa number of the pulp also increases, resulting in higher chemical costs in the bleach plant. Evaluated on this basis, an increase in the average kappa number by two units due to increased variability would result in approximately one million dollars a year in additional bleaching chemicals for a 1000 tonne/day mill. Furthermore, the use of excess bleach will increase the effluent toxicity, resulting in higher concentrations of toxins in the pulp and raising environmental concerns. Bleaching by itself is a very complex process, comprising of a multi-step procedure using numerous chemicals for pulp brightening, with the chemicals selected based on their economy and selectivity. Going into the details of bleaching is not in the context of this research, however it could be said with much confidence that greater uniformity in the digester should translate into chemical savings in the bleach plant.

Heterogeneous pulp coming from the digester will not only require higher bleach plant loadings to maintain the target brightness as explained above, but it will also cause complications in the downstream papermaking operations. Pageau and Davies [15] conducted a study on log sheets from various kraft pulp mills and compared the kappa coefficients of variability from the various unit operations in the mill. It was observed that variable pulp from the digester resulted in dramatically higher variability in the bleach plant chemical use; although, there was no strong relationship with the final pulp brightness. This was understandable since achieving uniform pulp with stable brightness is the key bleaching objective; however, with high heterogeneous

pulp coming from the digester, achieving the target brightness would be at the cost of complex complications and impaired ability of control in the downstream operating processes.

Pulp uniformity has also been correlated with pulp quality and strength on the basis of tear index and viscosity. MacLeod [16] conducted 12 triple-hanging-basket experiments in an industrial batch digester and measured the pulp kappa variability along the length of the digester. The pulp from each of the 12 trails was then tested for strength on the basis of tear index at a breaking length of 11 km, aiming to make a comparison between pulp uniformity and pulp strength delivery. For the trial that produced pulp with kappa variability of 7.8 units along the digester, the strength delivery values were 91 to 96%, whereas for the pulp with the lower kappa variability of 2.2 units, the strength delivery values increased to as much as 93 to 104%. With viscosity being another indicator of pulp strength delivery, Thompson and Gustafson [3] compared the viscosities of nonuniform pulps, with the same average kappa but different kappa distributions, based on the Tappi Test Method T230. The results showed that the control pulp (most uniform) had 36% higher viscosity than the poorly uniform mixture and 19% higher viscosity than the moderately uniform mixture. Hence, it could be deduced from these experiments that more uniform pulp from the digester would result in higher pulp strength deliveries.

Furthermore, higher kappa variability would result in higher heterogeneity in terms of over-cooked and under-cooked chips. This means that there would be a greater portion of pulp with very low kappa numbers that would suffer from blow damage and over-bleaching, translating into weaker pulp. Hence, it would be logical to postulate that the key to attaining pulp with superior strength would be to enhance the cooking uniformity within the digester. Ultimately, higher strength pulp would mean less pulp requirement for a given production of paper with the same base-paper quality, resulting in a multi-million dollar saving potential. The result of these studies have lead to the increased focus on the potential of more uniform pulp manufacture [10,17,18].

### 2.2.2 Sources of Kraft Pulp Variability

The nonuniformity of kraft pulp can arise from various sources at different scales. At the macro scale of the digester, variability may result from inhomogeneous or insufficient liquor flux and unequal temperature and/or chemical distribution within the digester. Consequently, this will lead to temperature and chemical concentration gradients throughout the interior space of the digester, producing nonuniform pulp [19]. Hypothetically, within-digester variance can be reduced through intimate chemical interaction of the wood chips and cooking liquor in a well-controlled temperature regime inside the digester. Yet, with the continued expansion in the size of modern digesters due to the increasing demand for pulp, achieving such conditions in the digester would be unrealistic [10].

At the chip-scale (or meso-scale), nonuniformity is caused by incomplete penetration, inadequate diffusion of the cooking liquor and temperature heterogeneities within the wood chips. Knots, oversized chips and dry chips may also result in intra-chip variability [20]. Experimental studies have shown that even if a fixed cooking program is followed, the lignin content of pulp varies with varying chip dimensions. The chip size, particularly chip thickness, can influence the rate of delignification and alkali consumption, resulting in nonuniform kappa distributions along the chip thickness. When pulping over-thick chips, the cooking is mass-transfer limited, with the rate of alkali consumption exceeding the rate of diffusion at pulping temperature. This would result in broad kappa distributions across the chip thickness, with the wood chips being over-delignified at the surface while the centres hold lignin concentrations corresponding to raw wood [18,21]. For this reason, wood chips with thicknesses greater than 8 mm are removed from the chip flow going into the digester and reprocessed (by rechipping/slicing/crushing) to smaller sizes [22]. Mill chips are commonly 3 to 5 mm thick. Use of thicker chips would result in uncooked cores giving higher residual lignin and screen rejects, while use of thinner chips would cause operational (e.g., blocked screens and hang-ups) and quality (weaker pulps) problems [23,24].

One of the pulping variables having considerable impact on uniformity both at the digester scale and at the chip scale is the temperature. At the digester scale, the cook temperature is exponentially proportional to the delignification rate and so even a small temperature gradient

along the digester would result in considerable pulp variability [25]. At the scale of a single chip, the cook temperature is proportional to the delignification rate and diffusion rate, such that with a 10°C increase in temperature, the delignification rate is approximately doubled whereas the diffusion rate increases only in proportion to the temperature. Hence, an increase in temperature would lead to faster delignification rates than the corresponding diffusion rates, resulting in the alkali in the chip centres being consumed by reaction faster than it could be replaced by diffusion. Hence, the chip centres would become more alkaline depleted, causing broader kappa distributions across the chip thickness, with well-cooked chip edges but undercooked chip centres [26]. For this reason, maintaining a uniform cook temperature throughout the digester interior space is fundamental for uniform pulp production.

However, even with the elimination of these intra-digester gradients and with the use of optimal sized wood chips, there may still be some underlying nonuniformity in the kraft pulp. These are the microscale sources of heterogeneity that occur on the single fibre scale and are more intrinsic to the wood itself. This hypothesis is further reinforced by the fact that truly uniform kraft pulp has never been observed even under carefully controlled, laboratory conditions. A study was conducted by Qiao and Gustafson [27] on the kraft pulping of miniature wood chips in a small laboratory-scale digester, under conditions that minimized the potential for mass transfer limitations on the reactions. In this work, variability in the lignin content was measured at the fibre level using a Fibre Kappa Analyzer (FKA). This device is a flow-through instrument that measures the fluorescence intensity of numerous kraft pulp fibres stained with Acridine Orange, which then correlates linearly with the kraft pulp kappa number, generating its kappa distribution. More details on this measurement method can be found in the work of Robinson et al [28]. The single fibre kappa distributions of the resulting pulps were then measured giving Gaussian kappa distributions with a coefficient of variation of 16%. This measurement confirmed the hypothesis on fibre-scale heterogeneity and gave a realistic limit for kappa uniformity. For comparison purposes, pulps produced under more typical pulping conditions using mill chips were then examined and the FKA results showed wider kappa distributions and higher kappa shoulders, presumably resulting from the more heterogeneous pulping conditions found in the commercial digesters, as opposed to that of the laboratory [27]. However, the main idea behind the FKA measurements was not to get exact quantitative data on lignin contents, but rather to provide an insight on the fibre scale pulp heterogeneity. The extent at which these FKA

measurements could be depended upon and whether they are actually a realistic representative of the pulp variability is still debatable [19].

## **2.3 Industrial Operations**

The kraft pulping process starts in the digester where the wood chips are subjected to cooking liquor comprising primarily of sodium hydroxide and sodium sulphide at elevated temperature and pressure. The liquor dissolves the lignin that binds the cellulose fibres together in the wood matrix, producing pulp. The kraft pulping process may occur in either a batch or a continuous digester system. After cooking, the pulp is separated from the undigested wood chips by screening and then washed to remove the spent cooking liquor. At this point, less than 10% of the lignin is remained in the pulp, which is then progressively removed through various stages of increasingly selective delignification and bleaching/brightening steps. This will not only remove the residual lignin but it will also whiten the fibres, after which they are pressed and dried into sheets [6].

Lignin removal in the digester is economically and ecologically more favourable than by the succeeding bleaching stages due to the large cost associated with the bleach chemicals and the increasing environmental concern regarding the pulp mill effluents. As a result, the driving force of present pulping technologies, regardless of whether it is conducted in batch or continuous manner, is to remove as much lignin as possible in the digester. This has led to various operational modifications in kraft digesters over the years. This section provides an overview of the batch and continuous digester systems and investigates the many modified cooking strategies that have been implemented for each pulping technique.

### **2.3.1 Batch Digesters**

In batch kraft cooking, the wood chips and cooking liquor are added simultaneously to the digester, which is then sealed and raised to the cook temperature to achieve the target lignin content. Typical temperature rise rates of 1 to 2 °C/min are attained during the heating phase of the cook and once the maximum cooking temperature of 160 to 175°C is attained, the wood chips and cooking liquor are reacted for 1 to 2 hours to achieve the target lignin content [29]. Essentially, there are two types of batch digester heating systems: with direct steam heating and

with indirect steam heating. The simplest means of direct steam heating is the injection of steam into the bottom of the digester vessel, with heat transfer throughout the digester column occurring by convection. This technique has the advantage of simplicity and rapid temperature rise; however, it suffers from cooking liquor dilution by condensate and nonuniform heating during a large part of the cook. A better practice adopts an indirect heating method with heat exchangers together with forced liquor circulation, improving the cooking uniformity within the digesters and eliminating cooking liquor dilution. Following the cook, the chips are then blown from the bottom of the digester, which usually has a conical section at its base for improved chip/pulp discharge [29]. Figure 1 shows a schematic of an indirectly heated batch kraft digester. Industrial batch digesters are cylindrical vessels 2.5 to 5 m in diameter, 8.5 to 19 m in height and 70 to 400 m<sup>3</sup> in volume.

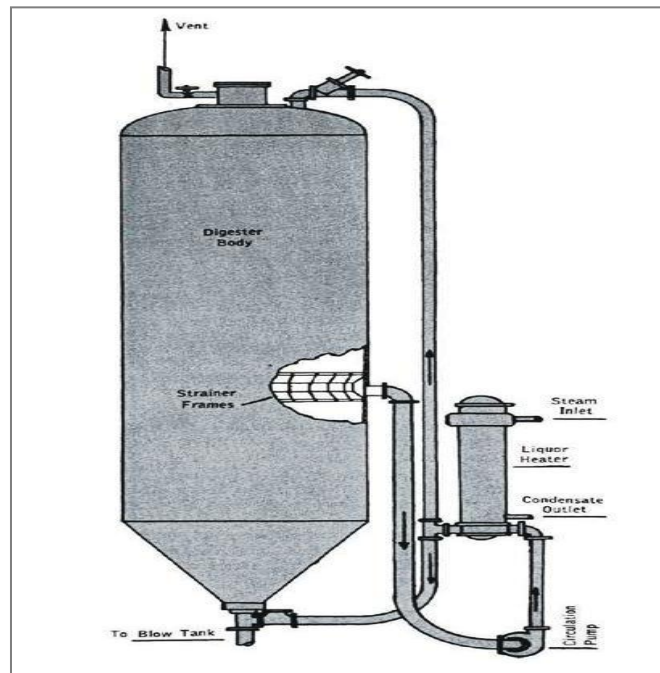


**Figure 1: Schematic of a Batch Digester with indirect steam heating**

The primary disadvantage associated with batch cooking was its relatively large energy consumption and so in the 1980s, this method of cooking experienced a renaissance following the introduction of the liquor displacement technique. This method involved charging the

digester with hot black liquor alongside the preheated white liquor, hence resulting in higher starting temperatures. Recent results show that displacement batch cooking is effective deeper into the wood chips (around 1 mm) than conventional cooking. Hence, this would reduce the amount of uncooked wood chips and lead to more uniform pulp production. Moreover, it would result in reduced steam consumption to about 50% of the conventional batch digester requirement and the increased size of the digesters by twice the volume of the conventional digesters [18,30].

### **2.3.2 Continuous Digesters**

The continuous kraft digester is a vertical tubular reactor in which the wood chips react with cooking liquor to remove the lignin from the cellulose fibres and produce pulp. Most continuous digesters consist of three basic zones: an impregnation zone, one or more cooking zones and a wash zone. The top of the digester is an impregnation zone where the chemicals penetrate and diffuse into the chips to ensure complete impregnation. Subsequently, the wood chips enter the cook zone where the delignification reactions occur and the majority of the lignin is removed, with liquor being added in either co-current or counter-current flow with respect to the wood chips (which is always going from top to bottom). The reaction is then stopped by the counter-current introduction of low temperature liquor into the lower region of the digester, referred to as the wash zone. Throughout the cooking process, the wood chips retain their original physical dimensions, until they reach the “blow” period at the end of the process where the individual fibres are liberated from the wood chips to produce pulp [31].

Conventional continuous digesters are either a single vessel or a two vessel system, comprising of the three zones explained previously, with the only difference that in the two vessel system the impregnation zone is a separate vessel by itself. Conventional cooking in continuous digesters means adding all the required white liquor within the chip feeding system, thus impregnation and cooking occur entirely in a co-current manner.

The objective of maximising lignin removal in conventional cooking would result in severe cellulose degradation in the yield and pulp quality [32]. Hence, over time, the continuous digester system has also gone through a series of modifications and improvements with techniques including: Lo Solids, Modified Continuous Cooking (MCC), Extended Modified

Continuous Cooking (EMCC) and IsoThermal Cooking (ITC). A schematic of an EMCC digester system is shown in Figure 2. All these methods are based on the principle that the alkali profile should be levelled out throughout the cook, that the hydrogen sulphide concentration should be high in the initial phase of the delignification process, and that the temperature should be kept as low as possible, especially in the beginning of the cook. This is achieved by having multiple white liquor inputs and black liquor extractions providing a more uniform alkali concentration over the entire cook. With the advent of the extended delignification era, much more is being demanded of the pulping systems, producing pulps with lower lignin contents (kappa numbers reduced by a third or more from traditional levels) as well as retained strength and yield [33, 34]. Industrial continuous digesters have total production capacities ranging from 200 to greater than 2000 air-dried tonnes per day of brownstock pulp, with the tallest vessel being 77 m, widest being 9 m and largest having a volume of approximately 4750 m<sup>3</sup> [35].

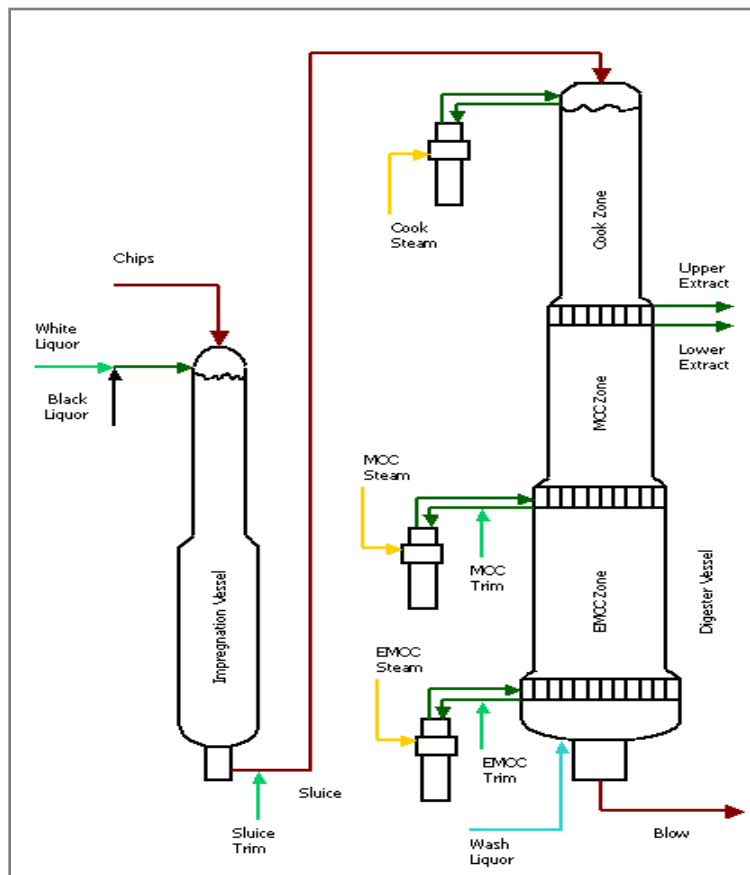


**Figure 2: Schematic of an EMCC System**

In today's kraft pulp production processes, batch and continuous digesters are both commercially being used. There is no great difference between the two digesters in the processing of any type, qualities of wood furnish, or in the pulp quality which can be produced [14]. However, for the production of moderate to high capacity pulp, the installation and operational costs would be lower when employing a continuous production unit [36]. Moreover, as with any continuous reactor system, the continuous digester is more space efficient, requiring less volume per unit retention time compared with batch [35]. On the other hand, batch digesters have the advantage of being more flexible with respect to grade changes and involve less complicated maintenance issues. Research work on batch digesters has been more profitable mainly because of the good accessibility to the insides of the digesters [10]. As explained in section 2.2, the growing demand for pulp has led to the continued increase in the size of digesters resulting in more heterogeneous pulp production – regardless of being a batch or continuous digester system. Having attained a clear picture of the two cooking techniques, the next chapter will provide a review of the various past approaches to measure the extent of variability within batch and continuous digester systems.

### **3. Review of Literature**

#### **3.1 Previous Works on Measuring Digester Variability**

Digesters play a significant role in shaping the pulp and paper qualities and the uniformity of pulping within them has become a key issue in optimising their performance. In the previous chapter, it was seen that uniform pulp production in the digester has many benefits for the economic and environmental performance of the pulping industry. For this reason, measuring variability within digesters has been a subject of intense investigation for many years. This chapter reviews the various past approaches and techniques that have been adopted for measuring the extent of delignification diversity within batch and continuous digesters.

##### **3.1.1 Batch Digesters**

Uniformity studies in a laboratory scale batch digester were conducted by Shomaly [37] in 1990 based on a “Layer Separation Technique”. The digester system under investigation was a 20L indirectly heated batch digester, charged with 2 kg of oven-dry wood chips and adopting pulping conditions similar to those of industry. The layer-separation technique offered a means of isolating six layers of wood chips inside the digester vessel and in so doing providing six pulp samples for kappa testing. Four cooks were conducted under equivalent pulping conditions using wood chips of thicknesses 2 to 6 mm and the kappa test results on the pulp samples for all the cooks gave an average kappa range of 1.2 units along the digester. Adding to this, a decreasing trend was observed in the lignin content of pulp when going down from the top layer to the bottom layer within the digester. This could be associated to variation in the liquor temperature, measured to be approximately 1.5°C along the digester. Also, the fact that the top layers were not completely immersed in liquor caused the higher kappa numbers at the top of the digester and this theory was further supported by the highly undercooked pulp that was observed at the top of the digester when the liquor circulation rate was turned off.

On an industrial scale, MacLeod [16] measured pulp variability as a function of position within a much larger batch digester based on a “hanging basket technique.” This was accomplished by isolating wood chips in hanging baskets at different positions along the digester to measure the extent of delignification diversity at the end of the kraft cook as a function of elevation in the

digester. The isolated chip samples were spaced approximately five meters apart along the vertical centreline of a well-controlled, indirectly heated batch digester and once the chips were pulped, they were retrieved for kappa analysis following the cook. Figure 3 presents the results from the hanging baskets showing the variation of kappa between the individual cooks, as well as the difference in the extent of reaction as a function of position in the digester for each cook. In each of the 12 mill cooks that were conducted, the kappa test results showed that there were significant differences in the extent of reaction as a function of position along the digester, with pulp variability ranging from 2.2 to 7.9 kappa units for a coefficient of variation of 5 to 16% - less uniform than that obtained in the smaller digesters. The higher uniformity within the laboratory scale system could be explained by the use of uniform chip dimensions (only chips with thicknesses 2 to 6 mm were employed) and carefully controlled digester conditions [37].

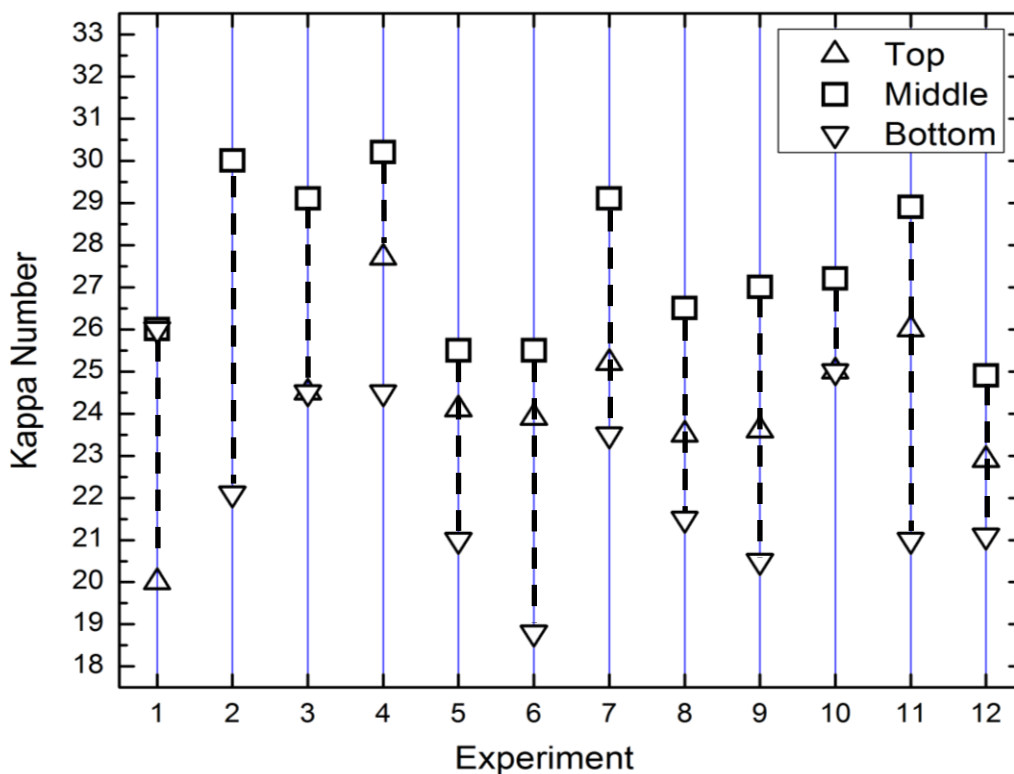


**Figure 3: Variation of kappa number as a function of location within an industrial batch digester based on the “triple-hanging-basket” technique reported by MacLeod [16].**

The hanging-basket technique cooks a known quantity of wood chips under industrial batch conditions, with the wood chips chosen from a master chip supply hence minimizing the heterogeneity caused by the raw material. Pulp variability along the digester has been attributed to insufficient or nonuniform liquor flow through the digester, resulting in temperature and/or liquor chemical concentration variations. In fact, this has been indirectly supported by the temperature measurements made on the exterior shell of the digester as a function of elevation - varying by as much as 4.5°C [38]. A clear positional pattern was also demonstrated from the hanging basket results, with the chips in the bottom basket always the most cooked (lowest kappa) and those in the middle basket always the least cooked (highest kappa). According to MacLeod [16], this was reasonable, since the liquor was hottest where it was introduced at the top and bottom of the digester as it had not yet exchanged its heat energy, while it was coolest and most depleted of alkali at the extraction screens in the centre.

With all this being said, the three hanging baskets were unable to represent the entire space inside a batch digester and in order to do that, one would have to fill the entire digester volume with hanging baskets. Adding to this, the temperature measurements that were made with the temperature probes mounted in the walls of the batch digester did not provide a clear picture of the actual temperature distribution throughout the mass of wood chips and liquor [39].

Pulp uniformity within industrial batch digesters has also been quantified by measuring the kappa variability at the digester exit during the blow period as a function of time. During digester discharge, chips from various locations of the digester exit the blow line and measurements of the kappa number of the pulp exiting the digester at intervals of one minute over a ten minute period were made, as shown in Figure 4 - giving a coefficient of variation of about 3.9%. This value was lower than the variability reported by MacLeod's hanging basket technique [16] because the pulp had been obtained from more of the digester volume (being more representative of the entire cook) and so some degree of mixing had been experienced by the pulp during its discharge [29].

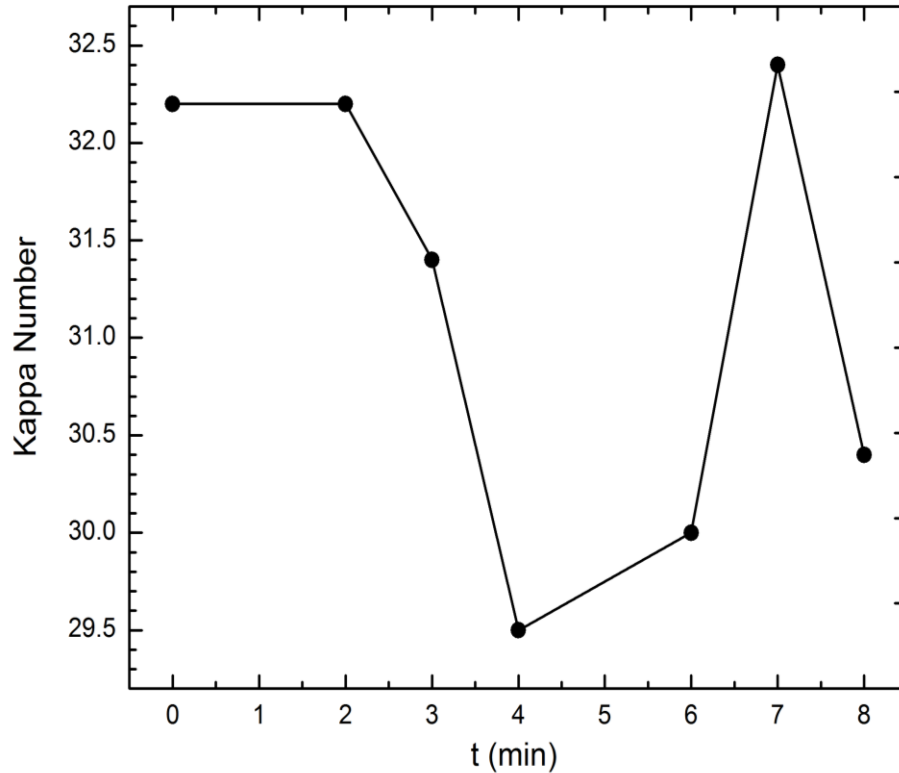


**Figure 4: Variation of kappa number at the digester blow line, as a function of time in an industrial batch digester as reported by Lee and Bennington [29].**

The previously explained experimental techniques demonstrate that pulp variability is related to liquor temperature gradients and nonuniform liquor flow through the digester. In order to achieve uniform pulp throughout the digester, each chip must experience the same time-temperature and time-liquor concentration history. Lee and Bennington [40] later used electrical resistance tomography (ERT) to evaluate the uniformity of liquor flow in a model laboratory batch digester scaled under industrial conditions. With the liquor introduction zones located at the top and bottom of the digester, no flow crossed the screen level. This resulted in a stagnation zone in the centre of the vessel, which also coincided with the point of highest kappa number reported by MacLeod [16] in the hanging basket experiments.

### 3.1.2 Continuous Digesters

Uniformity studies in continuous kraft digesters were primarily conducted by Hamilton in 1961 [1]. The literature reports this to be the only previous attempt to deploy a flow-following device through a continuous kraft digester. This involved tracing the passage of six radioactively-tagged chips through a small continuous digester using Geiger counters, with the tracer chips added one at a time, each flowing through the digester and then recovered prior to the addition of another chip to the system. The results from Hamilton's work confirmed the plug-flow motion of wood chips through the digester, observing that all chips came down in a vertical line with no spiralling or rotation. Moreover, thermocouples were used to measure the external surface temperature of the digester shell, hence attempting to correlate the temperature readings with the positional data so as to estimate the temperature-time profile experienced by the chips at various locations in the digester.

On an industrial scale, pulp kappa variability within continuous digesters was measured using online kappa number analyzers. Kubulnieks et al. [41] measured kappa variability at the digester blow line by means of an online STFI kappa number measurement system which was based on the ultraviolet light absorption by the lignin in the pulp. Based on these readings, a continuous fluctuation of 5 to 10% around the average was observed in the lignin concentration profile of the pulp [42]. Later, the online measurements were extended by Laitinen et al. [43] to measure the kappa number at the digester midpoint - right after the digester's cooking zone but before the washing zone. These readings provided insight on the heterogeneity within the digester and were also used for increasing control efficiency. Although, the results from these online measurements correlated well with the chemical kappa number analysis, large variations were seen in such short time-scales, which could not be satisfactorily discerned by traditional sampling and laboratory analysis. A possible explanation could be that the mixed stock may be masking a significant lignin content variation existing between the fibres [10].

Uniformity studies in industrial continuous digester systems were extended further by measuring kappa variability based on high frequency chemical kappa testing. Pulp samples were taken at half minute intervals from the blow line of an EMCC digester over a half hour period, collecting 72 pulp samples for kappa testing based on the TAPPI T-236 cm-85 test method. The results are

shown in Figure 5 and as it can be seen, the kappa variability fell within 32 to 37 units with a variance of 1.1 kappa units and a coefficient of variation of 3.3%. A better illustration of the kappa distribution within the digester was established by the construction of a histogram based on the kappa readings, as shown in Figure 6. Kappa variability within the digester closely resembled a Gaussian distribution, showing that the kappa distribution was a bell shaped curve that was more concentrated around the mean, with lower tendency to produce the unusually extreme values [44].

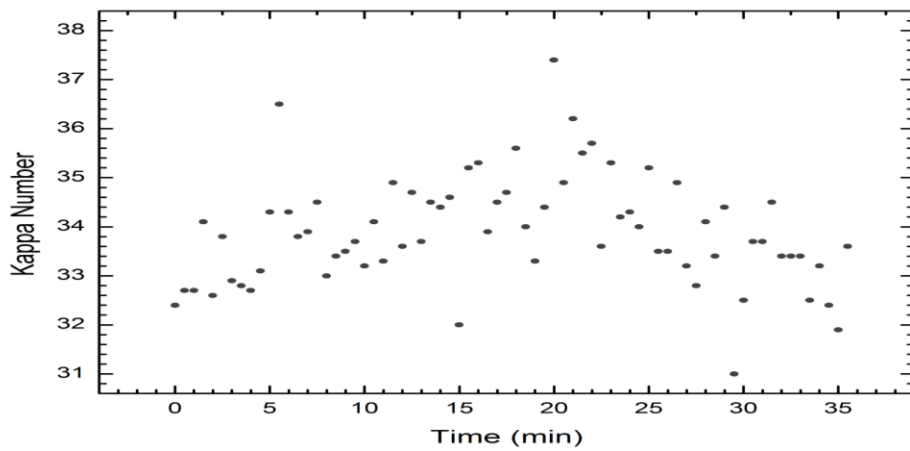


**Figure 5: Kappa variation in an Extended Modified Continuous Cooking System with chemical kappa testing on 72 pulp samples taken at the digester blow line at 30s intervals over a half hour period.**

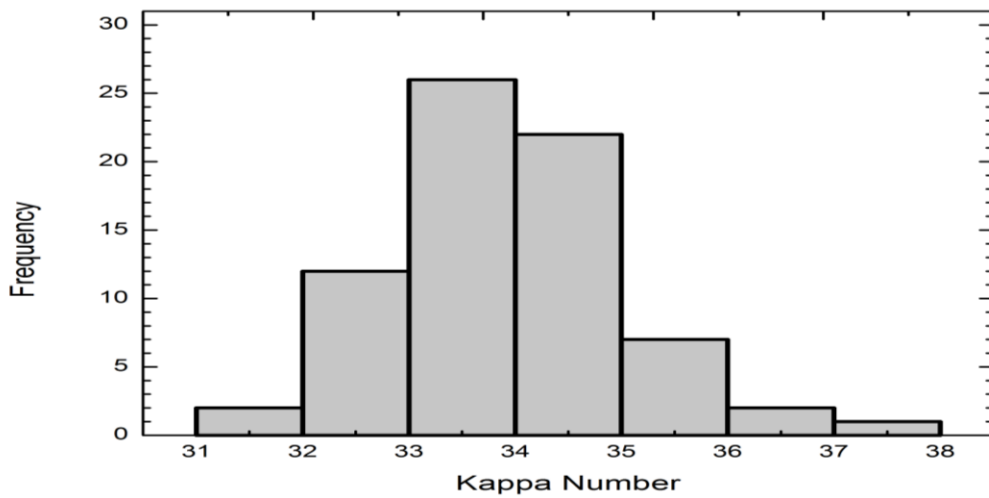


**Figure 6: Histogram of the kappa distribution in the EMCC system based on the results from Figure 5.**

With all this being said, the fact that pulp samples taken from a tiny hole inside the digester wall could give any reliable information on what was happening elsewhere inside the digester was still questionable, regardless of whether the pulp kappa was determined online by kappa analyzers or through chemical testing in the laboratory. The limitation on these measurements was that they were taken from a fixed location within the digester. In order to provide a better picture of the extent of variability in the digester space, one would need more sampling points inside the digester. This would mean making more holes in the digester and hence translating into higher costs. All the techniques developed thus far are sufficient for control purposes, although they may not provide a clear picture of what is actually going on inside the continuous digester systems and the extent of variability throughout the mass of chips and liquor in the digester.

To put it briefly, this chapter has detailed an investigation on the various past approaches that have been adopted for measuring the extent of delignification diversity within batch and continuous digester systems. Thus far, data in this area is rather limited in the sense that the variability within the digester is not known both throughout the entire digester space and at all times during the cook period, i.e., MacLeod's [16] hanging baskets in the batch digester system measured kappa variability at various elevations along the digester but only at the end of the cook, and Andrew's [44] kappa variability studies in the continuous digester system measured the kappa variability at various time intervals during the cook but only at the digester blow line. Hence, this has motivated the development of a new method for measuring variability within the digester: the "SmartChip". This device measures and records various parameters including the temperature directly inside the digester while experiencing the same conditions as the wood chips during the kraft cook. More details on the SmartChip are provided in the succeeding chapters.

## 4 Modeling Heat Transfer in Kraft Digesters

In the kraft pulping process, strong interactions through mass, momentum and energy exchanges occur between the wood chips and cooking liquor in the digester. The result of pulping is dependant on a great number of variables, as discussed in Section 2.2.2, however, the most important is arguably the temperature variability within the digester. This chapter looks into the impact of temperature distribution on the pulp properties, and then develops a model for understanding the heat transfer mechanisms occurring inside the digester during the kraft cook.

### 4.1 The Significance of Temperature in Pulping Kinetics

One of the earliest, simplest and still widely used models describing kraft pulping kinetics is the “H-factor” developed by Vroom [25] in 1957. This model is based on a time-temperature study of the pulping process, integrating these variables into a single variable referred to as the H-factor and evaluated according to Equation (1). The H-factor is used to represent the extent of cooking during the kraft process, based on the assumption that an increase in cooking temperature would result in an Arrhenius-type rate increase in the wood substance removal from the pulped chips.

$$H = \int_0^t \exp \left[ \frac{-E_a}{R} \left( \frac{1}{T(t)} - \frac{1}{373} \right) \right] dt \quad (1)$$

In Equation (1),  $E_a$  is the activation energy, typically 134 kJ/mol for the kraft process,  $R$  is the ideal gas constant and  $T$  is the absolute temperature at a given time during the cook. Many studies have been conducted to relate the H-factor to the properties of the pulp produced. A model has been developed by Hatton [45], to predict the kappa number of the pulp based on the H-factor, the initial effective alkali content of the liquor,  $EA$ , and constants that are determined based on the wood species  $\alpha$ ,  $\beta$  and  $n$  – as shown in Equation (2).

$$K = \alpha - \beta \left[ (\log_{10} H)(EA)^n \right] \quad (2)$$

The above-mentioned equations relate the cooking time and temperature to the pulp properties and show the impact of temperature variability on the pulp produced. It is evaluated from the

exponential relationship between temperature and pulping reaction rate, that with only a 2°C variation along the digester, there would be  $\pm 8\%$  variability in the accumulated H-factor of the pulp while cooking the chips for two hours at the maximum pulping temperature of 170°C. Moreover, for the Hemlock wood species used in this work, this would translate into a kappa variability of 5 units by the end of the cook. Hence, it is shown that temperature gradients along the digester will produce pulp with a broad kappa distribution, highlighting the importance of minimizing temperature variability for uniform pulp production.

## 4.2 Model Development

This section focuses on the development of a model describing the heat transfer processes occurring in the digester during the kraft cook. We begin the analysis by describing the geometry of the system under study. A cylindrical 5L M/K laboratory batch digester is filled with wood chips and cooking liquor - its basic configuration and dimensions are shown in Figure 7. The digester is indirectly heated with the hot liquor entering the top opening of the digester at a flow rate of 3L/min and then flowing down the digester and exiting through the bottom where it is reheated in a heat exchanger and returned back to the top of the digester.

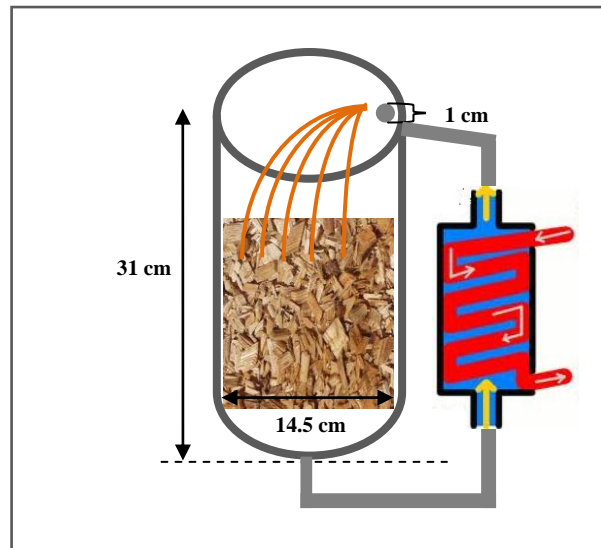


**Figure 7: Schematic of the 5L M/K batch digester system, showing the dimensions and geometry of the digester for modeling the heat transfer processes occurring within it.**

Due to the porous structure and non-homogeneous nature, thermal transport in the wood is rather complex [46]. The model development starts by describing the heat transfer process in the form of the conservation of energy equation based on the first law of thermodynamics. Equations (3) and (4) show the volume-averaged energy balances for the solid (wood) and fluid (liquor) phases respectively. The model is developed under cylindrical coordinates, however, radial and tangential uniformity within the digester have been assumed, simplifying the equations into a one-dimensional analysis. Adding to this, radiative effects, viscous dissipation and work done by pressure changes are neglected. In Equations (3) and (4) the subscripts  $s$  and  $f$  refer to the solid and fluid phases respectively,  $T$  is the temperature,  $t$  is the time,  $\rho$  is the density,  $c_p$  is the isobaric specific heat capacity,  $\varphi$  is the porosity,  $k$  is the thermal conductivity,  $v$  is the velocity of the fluid phase,  $h$  is the interphasial heat transfer coefficient and  $q''$  is the internal heat source. As it can be seen from these equations, the temperature distribution in the digester results from the constituent energy fluxes in the process: heat transfer by conduction, heat transfer by convection, heat transfer between the solid and fluid phases and heat production [47].

$$(1 - \varphi)(\rho c_p)_s \frac{\partial T_s}{\partial t} = (1 - \varphi) \frac{\partial}{\partial x} \left( k_s \frac{\partial T_s}{\partial x} \right) + h(T_f - T_s) + (1 - \varphi)q_s'' \quad (3)$$

$$\varphi(\rho c_p)_f \frac{\partial T_f}{\partial t} + (\rho c_p)_f v \frac{\partial T_f}{\partial x} = \varphi \frac{\partial}{\partial x} \left( k_f \frac{\partial T_f}{\partial x} \right) - h(T_f - T_s) + \varphi q_f'' \quad (4)$$

Further simplification of the two-equation model could be established by assuming that the solid and fluid phases constituting the porous media are in thermal equilibrium, such that  $T = T_s = T_f$ . According to Truong and Zinsmeister [48] this assumption is only valid if the thermal conductivities of the two constituents do not differ widely. Besides, it is also assumed that the heat conduction in the solid and fluid phases take place in parallel such that there is no net heat transfer from one phase to another [47,49]. Hence, thermal transport is described by a single local temperature,  $T$ , combining Equations (3) and (4) into the one-equation model shown in Equation (5) – with the subscript  $m$  representing the porous medium (both solid and fluid phase).

$$(\rho c_p)_m \frac{\partial T}{\partial t} + (\rho c_p)_f v \frac{\partial T}{\partial x} = k_m \frac{\partial^2 T}{\partial x^2} + q'' \quad (5)$$

where Equations (6) to (8) represent the overall heat capacity per unit volume, overall thermal conductivity, and overall heat production per unit volume of the porous medium, respectively.

$$(\rho c_p)_m = (1 - \varphi)(\rho c_p)_s + \varphi(\rho c_p)_f \quad (6)$$

$$k_m = (1 - \varphi)k_s + \varphi k_f \quad (7)$$

$$q'' = (1 - \varphi)q_s'' + \varphi q_f'' \quad (8)$$

Another simplification applicable to this model would be to assume that the local accumulation of heat of reaction is negligible. The kraft pulping process is accompanied by a slight exothermic heat of reaction, which is very small in comparison to the amount of heat input for the temperature rise – constituting about 8% of this heat input. On the other hand, the convective heat loss from a laboratory scale digester to the surrounding constitutes about 9% of the amount of heat input for the temperature rise. As a result, the heat of reaction could essentially be compensated for by the heat loss [50] and so we set  $q'' = 0$ . After these simplifications, the one-equation model describing heat transfer along the digester is given by Equation (9) and can be solved together with the initial and boundary conditions given in Equations (10) to (12).

$$(\rho c_p)_m \frac{\partial T}{\partial t} + (\rho c_p)_f v \frac{\partial T}{\partial x} = k_m \frac{\partial^2 T}{\partial x^2} \quad (9)$$

At the beginning of the cook, the digester contents are assumed to have uniform temperature at ambient conditions,  $T_a$ , as given in Equation (10). At the top of the digester where the liquor is first introduced, the temperature profile of digester contents is equivalent to the predefined temperature schedule of the heated liquor,  $T_p$ , as given in Equation (11). While traveling down the length of the digester, the contents lose some of the heat and by the time the liquor reaches the bottom of the digester, it has minimum temperature. Hence, the zero heat flux condition is used at the bottom of the digester, as given in Equation (12).

$$t = 0 \quad T = T_a \quad (10)$$

$$x = 0 \quad T = T_p(t) \quad (11)$$

$$x = 1 \quad \frac{\partial T}{\partial x} = 0 \quad (12)$$

The partial differential equation given in (9) is scaled prior to obtaining the solution so as to provide a constructive method to formulate the model in terms of dimensionless quantities and it is presented by Equation (13). The dimensionless parameters in this equation are  $T^*$ ,  $t^*$  and  $x^*$  and are solved by Equations (14) to (16) respectively, with  $L$  being the vertical length of the digester,  $T_{max}$  being the maximum cook temperature and  $t_a$  being the advective time scale. The advective time scale is described as the time it takes the fluid to travel down the length of the digester, provided that the velocity of the liquor traveling through the porous media,  $v$ , is known. The initial and boundary conditions are also scaled accordingly, as given in Equations (17) to (19).

$$\left[ \frac{(\rho c_p)_m L^2}{t_a k_m} \right] \frac{\partial T^*}{\partial t^*} + \left[ \frac{(\rho c_p)_f v L}{k_m} \right] \frac{\partial T^*}{\partial x^*} = \frac{\partial^2 T^*}{\partial x^{*2}} \quad (13)$$

$$x^* = \frac{x}{L} \quad (14)$$

$$T^* = \frac{T - T_a}{T_{max} - T_a} = \frac{T - T_a}{\Delta T} \quad (15)$$

$$t^* = \frac{t}{t_a} \quad \text{where} \quad t_a = \frac{L}{v} \quad (16)$$

$$t^* = 0 \quad T^* = 0 \quad (17)$$

$$x^* = 0 \quad T^* = 1 \quad (18)$$

$$x^* = 1 \quad \frac{\partial T^*}{\partial x^*} = 0 \quad (19)$$

### 4.3 Thermo-physical Properties of Wood

The successive step involves evaluating the thermo-physical properties of the wood required for solving the heat transfer model in Equation (13). Some of these properties may be influenced by the type of wood specie being used or variables like the moisture content, whereas others may be independent of species. The density ( $\rho_s$ ), specific heat ( $c_p$ )<sub>s</sub>, and thermal conductivity ( $k_s$ ) of the moist wood required for the solution of Equation (13) are calculated using the relations proposed by Simpson and TenWold [51].

#### 4.3.1 Density

The density of wood depends greatly on its moisture content as it contributes to part of the weight of the wood and therefore the density must reflect this fact. The density of the moist wood is evaluated based on Equation (20),

$$\rho_s = 1000G_m(1 + M/100) \quad (kg/m^3) \quad (20)$$

where  $M$  is the moisture content of the wood (in %), which represents the weight of water in wood expressed as a percentage of the weight of oven-dry wood and  $G_m$  is the specific gravity based on volume at moisture content  $M$ . This could be calculated based on Equation (21), where  $G_b$  is the specific gravity based on the green volume and  $a = (30-M)/30$ , for  $M < 30$ . Here the density of wood is assumed to be constant and independent of the type of wood.

$$G_m = G_b / (1 - 0.265aG_b) \quad (21)$$

#### 4.3.2 Specific Heat Capacity

The heat capacity of wood is dependant on the temperature and the moisture content of the wood. The heat capacity of dry wood is roughly correlated to temperature (in Kelvins) by the relation given in Equation (22). With the heat capacity of the moist wood being greater than that of dry wood, there is an additional adjustment factor,  $A_c$ , which accounts for the additional energy in the wood-water bonds, as given in Equation (23). The adjustment factor could be

evaluated based on Equation (24), with the constants given as  $b_1 = -0.06191$ ,  $b_2 = 2.36 \times 10^{-4}$ ,  $b_3 = -1.33 \times 10^{-4}$ .

$$c_{p,s0} = 0.1031 + 0.003867T \quad (22)$$

$$(c_p)_s = \frac{c_{p,0} + 0.01Mc_{p,w}}{1 + 0.01M} + A_c \quad (kJ/kg K) \quad (23)$$

$$A_c = M(b_1 + b_2t + b_3M) \quad (24)$$

### 4.3.3 Thermal Conductivity

The thermal conductivity of the wood is reflected by the density, moisture content and many other properties of the wood. For woods which the moisture content is below 25%, the approximate thermal conductivity could be evaluated based on the linear relation given in Equation (25), where the constants  $A$ ,  $B$  and  $C$  have values  $0.01864$ ,  $0.1941$  and  $0.0004064$  respectively.

$$k_s = G_m(B + CM) + A \quad (W/m K) \quad (25)$$

By calculating the thermo-physical properties of moist wood based on the equations given in this section and by assuming that the liquor has the same thermo-physical properties as water, then we could evaluate the overall heat capacity,  $(\rho c_p)_m$  and the overall thermal conductivity,  $k_m$  for the medium based on Equations (6) and (7).

## 4.4 Model Solution

The heat transfer equation describing the temperature distribution of the digester contents during the kraft cook is given in Equation (26). This equation could be solved based on the initial and boundary conditions specified in Section 4.2.

$$\frac{\partial T^*}{\partial t^*} + \lambda \frac{\partial T^*}{\partial x^*} = \varepsilon \frac{\partial^2 T^*}{\partial x^{*2}} \quad (26)$$

where  $\lambda = \frac{\left[ \frac{(\rho c_p)_f v L}{k_m} \right]}{\left[ \frac{(\rho c_p)_m L^2}{t_a k_m} \right]} = \frac{(\rho c_p)_f}{(\rho c_p)_m} \cdot \frac{v t_a}{L} = \frac{(\rho c_p)_f}{(\rho c_p)_m}$

$$\varepsilon = \frac{1}{\left[ \frac{(\rho c_p)_m L^2}{t_a k_m} \right]} = \frac{1}{(\rho c_p)_m} \cdot \frac{t_a k_m}{L^2}$$

The solution to equation (26) requires solving for the values of  $\lambda$  and  $\varepsilon$  - evaluated based on the thermo-physical properties of wood (equations (20) to (25) in Section 4.3) and the dimensions of the digester system under study (specified in section 4.2). This model is solved in Chapter 7 and the theoretical predictions from the model are then compared with the experimental results of the SmartChip data.

## 5 The “SmartChip”

The demand for increased pulp production capability has led to an increase in the size of modern digesters – principally through larger vessel diameters [2]. While this has lowered the unit cost of a tonne of pulp, it has increased the risk of pulp variability and highlighted the need to collect data from within the digesters so as to evaluate the extent of variability within them. Chapter 3 provided a review of the various past approaches to measure the extent of delignification diversity within digesters and Chapter 4 emphasized on the significance of temperature variability on pulp properties. As pointed out in Chapter 3, most temperature data from within industrial digesters are collected from temperature probes mounted in thermowells in the wall of the digester, or sensors mounted at the digester inlet or outlet [39]. While these techniques are sufficient for control purposes, they fail to provide a clear picture of the temperature distribution throughout the mass of chips and liquor in the digester. Improving the coverage by adding more sensors is possible but the cost would be prohibitive and the harsh environmental conditions within the digesters would increase the difficulty of making reliable temperature readings. Hence this has motivated a new method of measuring digester variability: the SmartChip.

### 5.1 The “SmartChip” – What is it?

A flow-following sensor package or “SmartChip” – shown in Figure 8, has been developed for use in kraft digesters to collect data from within the process. The SmartChip is a small (approximately 7.5 cm in diameter), robust, self-powered sensor platform that mimics the behaviour of the wood chips through the process and records the temperature within the digester during the kraft cook. Each SmartChip has two temperature sensors (namely the I-RTD sensor and the E-RTD sensor) that are spaced approximately 5 cm apart. The onboard sensors will collect time/temperature data from within the digester directly and then store this data in a non-volatile memory. If the SmartChip is flowing through the digester, then at the digester exit, the wood chips will reach the fibre liberation point and will be readily defibred, while the SmartChip, in contrast, will remain intact and could be separated from the pulp stream along with the other undigested material as part of normal processing operations. Once the SmartChip has been retrieved, the complete sensor data log stored in the memory could be downloaded and analyzed.

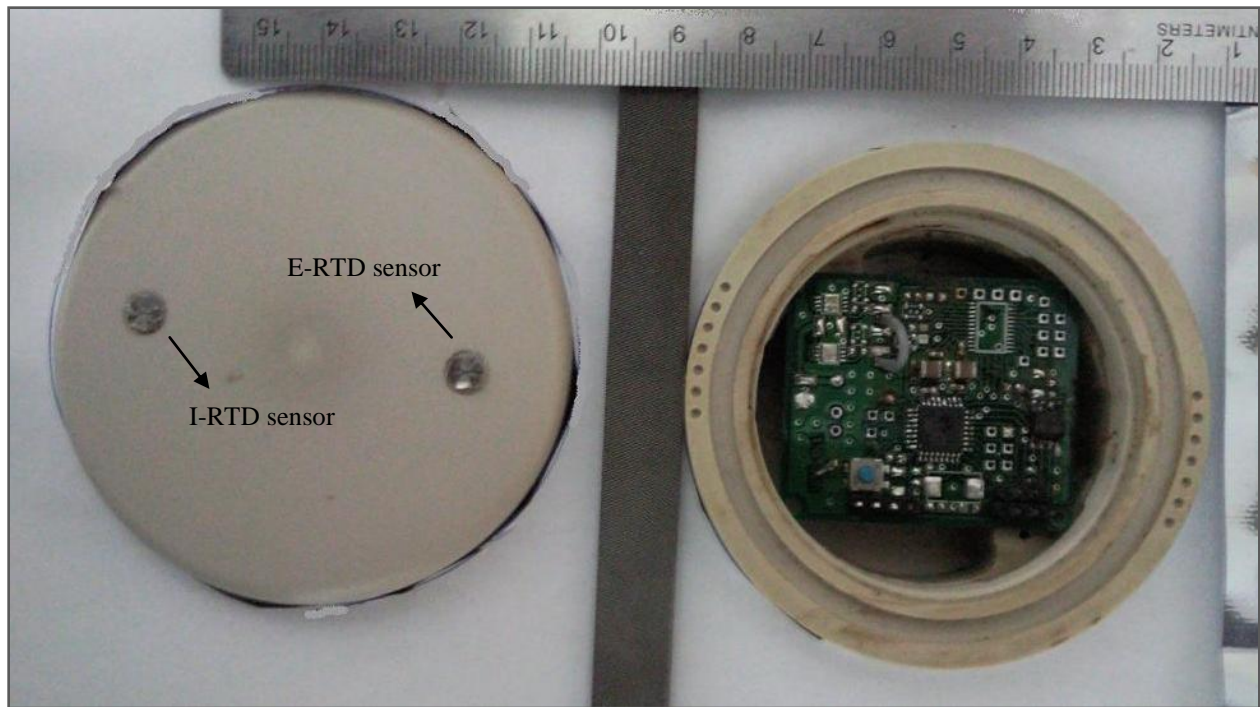


**Figure 8: A photograph of two SmartChips – one to show the SmartChip electronics and another to show the alignment of the sensors on the outside. The SmartChip package has a diameter of approximately 7.5 cm.**

The inside of the kraft digester is a rather harsh environment, comprising of highly alkaline solutions of primarily NaOH and Na<sub>2</sub>S and temperatures as high as ~170°C, with the digester contents kept at these conditions for several hours to achieve the required degree of delignification. It is essential that the SmartChip can survive this environment during its journey through the digester. Moreover, there are numerous mechanical obstacles in the digester that the SmartChip may encounter, and so it must be designed in a way that not only it survives them, but it also has minimal impact on digester operation.

The SmartChip's recorded time/temperature data could then be used to provide insight on the temperature variability within the digester and predict the pulp properties based on the equations provided in Section 4.1. The use of a single SmartChip in several cooks would provide information on the range of cooking conditions experienced in independent cooks, whereas the use of multiple SmartChips in a single cook would evaluate the extent of heterogeneity within the digester. The results from the SmartChip digester trials are presented in Chapter 7.

## 5.2 The “SmartChip” Components

The ultimate long-term objective of this project is the development of a SmartChip that mimics the flow of the wood chips through the digester and has dimensions and density similar to that of the wood chips. However, prior to this, a prototype SmartChip has been made so as to set the foundation for its further improvement. The device being used to collect the data being presented in this thesis is the prototype SmartChip shown in Figure 8 and the objective of this section is to give a brief review of its comprising design components.

The SmartChip is packaged in a way that it has a density close to that of liquor saturated wood chips and can withstand 2 MPa at 180°C in a highly caustic environment. Initially, a  $10 \times 6 \text{ cm}^2$  screw-top cylindrical Polytetrafluoroethylene (PTFE) package was constructed. This package was able to withstand the digester conditions and was easily machinable, but had a fairly high density and low strength. To compensate for this, the packaging was redesigned through the use of a Polyether ether ketone (PEEK) package having dimensions  $7.5 \times 4 \text{ cm}^2$ , a density closer to that of liquor saturated wood chips and a higher strength. This allowed for the decrease in the package size, however, it was more expensive and more difficult to machine. Digester trials with both SmartChip packages have been conducted and the results are presented in Section 7.1.

Inside the package, the SmartChip consists of three main design components: electronics, power supply and sensors - as shown in Figure 9. The electronics are positioned at the heart of the SmartChip and comprise of a microcontroller, analog-to-digital converter (ADC), clock and memory. The electronics are responsible for optimizing the power consumption, controlling the data acquisition, signal conditioning and data handling. With regards to power, the SmartChip must survive for at least eight hours during its transit through the continuous digesters. With the power consumption of the electronics and temperature sensor in the prototype SmartChip being approximately 2 mA in sleep mode and 4 mA in active mode and with a sampling rate at every 30s, the battery chosen for this work is predicted to provide power for ~270 hours of continuous operation, enough for ~30 trips through a continuous digester [52].

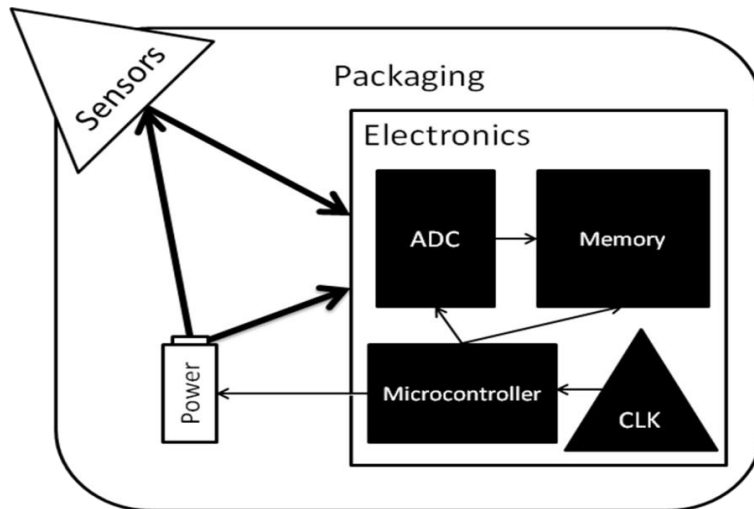


**Figure 9: Block Diagram of SmartChip prototype components and the communication between them.**

The SmartChip comprises of two temperature sensors: I-RTD and E-RTD as shown in Figure 8. The temperature sensor chosen for the SmartChip is a resistance temperature detector (RTD) mounted in direct thermal contact to the digester environment. The accuracy of the temperature sensor is particularly important due to the exponential relationship between the reaction rate and temperature. An uncertainty of just  $\pm 1^\circ\text{C}$  over a 2 hour cook is compounded to an error as large as 8% in accumulated H-factor.

The absolute accuracy of the SmartChip temperature readings is a function of sensor accuracy and electronic precision. The stability of the electronics over the complete cooking temperature range is critical in maintaining accuracy. The accuracy of the SmartChip temperature readings was found to be  $\pm 0.3^\circ\text{C}$  with an offset of  $-0.95^\circ\text{C}$ . Careful design and calibration of the SmartChip electronics were shown to improve the accuracy of these reading to  $\pm 0.1^\circ\text{C}$ . Sensor accuracy refers to the relative accuracy of the sensors against one another so as to ensure that they read the same temperature. The SmartChip temperature sensor chosen is a thin-film  $1000\Omega$  class-A platinum RTD, model F2020 from Omega.ca, having a tolerance of  $\pm 0.15 + 0.002T^\circ\text{C}$ , giving sensor accuracy of  $\pm 0.51^\circ\text{C}$  at  $180^\circ\text{C}$ . Hence, the absolute accuracy of the SmartChip temperature measurement is  $\pm 0.52^\circ\text{C}$  at  $180^\circ\text{C}$ , calculated from the calibrated precision of the

electronics and the accuracy of the RTD sensor. More details on the calibration procedure are given in Appendix C.

With regards to the SmartChip timekeeping, a watchdog timer of the microcontroller is employed. The watchdog timer oscillates at a frequency of 125 kHz at 25°C and interrupts are used to control the sampling interval. The temporal error would amount to 18 minutes in 4 hours, however, calibration can compensate for this, reducing the error to 46s in a 4 hour period - the details of time calibration are also presented in Appendix C. Having introduced the SmartChip, its development and its design components, the subsequent chapters will focus on the application of the SmartChip inside the kraft pulp digesters.

## **6 Experimental Methods**

The experimental work of this thesis involves the deployment of a single SmartChip in several cooks to provide information on the range of cooking conditions experienced in the independent cooks and multiple SmartChips in a single cook to evaluate the extent of heterogeneity and the heat transfer mechanism occurring within the digester. This chapter describes the experimental methods for each digester trial that was conducted: the digester system being used, the cook specifications and the SmartChip(s) alignment.

### **6.1 Single SmartChip Testing**

Preliminary testing of the SmartChip involved ensuring that it could withstand the harsh conditions of the kraft cook and that it would measure and record the time/temperature data within the digester during its transit. These tests were done in a 5L M/K laboratory batch digester, loaded with 480 g of oven-dry pine wood chips and a single SmartChip placed in the centre of the digester. Figure 7 in Chapter 4 showed a schematic of the digester system being used and its dimensions. The digester had the capacity to encompass 500 g of oven-dry wood chips, but considering the volume occupied by the SmartChip, this amount had to be reduced down slightly. The wood chips were reacted with 2.46 litres of white liquor (effective alkali charge of 18% on wood and sulphidity of 30% - prepared based on the procedure explained in Appendix A), to give a liquor-to-wood ratio of 7.5 L/kg o.d. A rather high liquor-to-wood ratio was used in this laboratory-scale digester to ensure that all the wood chips were fully covered with liquor. The total liquor flow through the liquor circuit was kept at 3 L/min, and a sensor was mounted in the liquor circulation loop to measure the temperature of the liquor discharged from the vessel prior to heat up. The digester contents were heated at a rate of 1.5°C/min to a target cook temperature of 170°C and the time at which the contents were kept at cook temperature was within the range of 150 – 190 minutes.

Several trials with varying time-at-cook temperatures were conducted with a single SmartChip so as to provide information on the range of cooking conditions experienced in the independent cooks. This was done by taking pulp samples from the vicinity of the SmartChip sensor for kappa testing at each cooking trial. The cooked wood chips were prepared for kappa testing by

cooling with fresh water, disintegrating for five minutes by agitation and then washing in a vibrating flat screen having 0.38 mm slots. The accepts were then used to measure the kappa number of the pulp based on the half kappa tests [53] – procedure of this test is explained in Appendix B. Section 7.1 presents the results from these preliminary experiments.

## **6.2 Multiple SmartChips in a Single Cook**

Having experimented that the SmartChip is able withstand the harsh conditions of the kraft cook and that it is robust for use in the digesters, this section concentrates on evaluating the variability within the digesters through the deployment of multiple SmartChips.

### **6.2.1 Multiple SmartChips in 5L M/K Batch Digester**

In this trial, two SmartChips were positioned approximately 20 cm apart in the vertical centreline of the 5L M/K laboratory batch digester, loaded with pine wood chips and cooked under the exact same cooking conditions as in Section 6.1. The digester contents were heated at a rate of 1.5°C/min to a cook temperature of 170°C and the time-at-cook temperature was 165 minutes. The results from this trial are presented in section 7.2.

### **6.2.2 Multiple SmartChips in 20L Batch Digester**

As discussed in earlier, pulp variability has become more of an issue with the increasing size of digesters and so the testing has been extended to a larger, 20L batch digester. The digester vessel has a height of 74 cm and an internal diameter of 21.5 cm, loaded with 3 kg of oven-dry hemlock wood chips (accepts 2 mm to 4 mm) reacting with white liquor (effective alkali charge of 17% on wood and sulphidity of 26.95%), to give a liquor-to-wood ratio of 4.5 L/kg o.d. – similar to the conditions used in the mill. The cook profile had a ramp rate of 1.11°C/min to a cook temperature of 170°C and the cooking time was determined by the target H-factor. The liquor flow through the liquor circuit fluctuated between 10 to 16 L/min, and two temperature sensors were mounted at the top and bottom of the digester - the top sensor was mounted after the heat exchanger to measure the temperature of the heated liquor prior to its discharge into the vessel and the bottom sensor was mounted prior to the heat exchanger to measure the temperature of the liquor just after leaving the digester. The two SmartChips were placed at the top and bottom of

the digester vessel approximately 34 cm apart and both were surrounded by wood chips. The SmartChip measurements could then be used to give some idea of the axial temperature distribution along the digester.

Moreover, to establish a correlation between pulp variability and the temperature distribution within the digester, pulp samples were taken from the vicinity of the SmartChip sensors for kappa testing. The cooked wood chips were prepared for kappa testing by cooling with fresh water, disintegrating for five minutes by agitation and washing in a vibrating flat screen having 0.38 mm slots. The accepts were then used to measure the kappa number of the pulp at the various positions along the digester based on the half kappa tests [53] – explained in Appendix B. Moreover, each kappa measurement had one replicate to evaluate the precision of the measurement method and to ensure that it satisfies the TAPPI standard of 1.5% repeatability.

To effectively show the correlation between temperature gradients and kappa variability, every effort was made to minimize other potential causes of pulp nonuniformity. Previous experiments [21] have shown that chip thickness greatly influences the pulping rate, with the small-sized chips overcooked and the large-sized undercooked. Therefore, uniformly sized wood chips were screened (accepts of 2 to 4 mm) for use in all cooks, so as to minimize the variability arising from chip size distribution – this has already been discussed in Section 2.2.2. Furthermore, cook-to-cook variability is also reduced by keeping all the experimental parameters consistent for all the individual cooks. The results from the SmartChip trials in the 20L digester are presented in Section 7.3.

## 7 Results and Discussions

### 7.1 Single SmartChip Testing

A single SmartChip (initially one with a  $10 \times 6 \text{ cm}^2$  PTFE package) was positioned in the centre of the 5L M/K laboratory batch digester under the conditions specified in Section 6.1. As discussed earlier, the objective of this experiment was to ensure that the SmartChip could withstand the harsh conditions of the kraft cook. The digester also had a temperature sensor mounted in the liquor circulation loop at its bottom prior to the heat exchanger, to measure the outlet temperature of the liquor after leaving the digester and prior to being heated up. The temperature profile recorded by the SmartChip and the digester sensor at the outlet are presented in Figure 10.

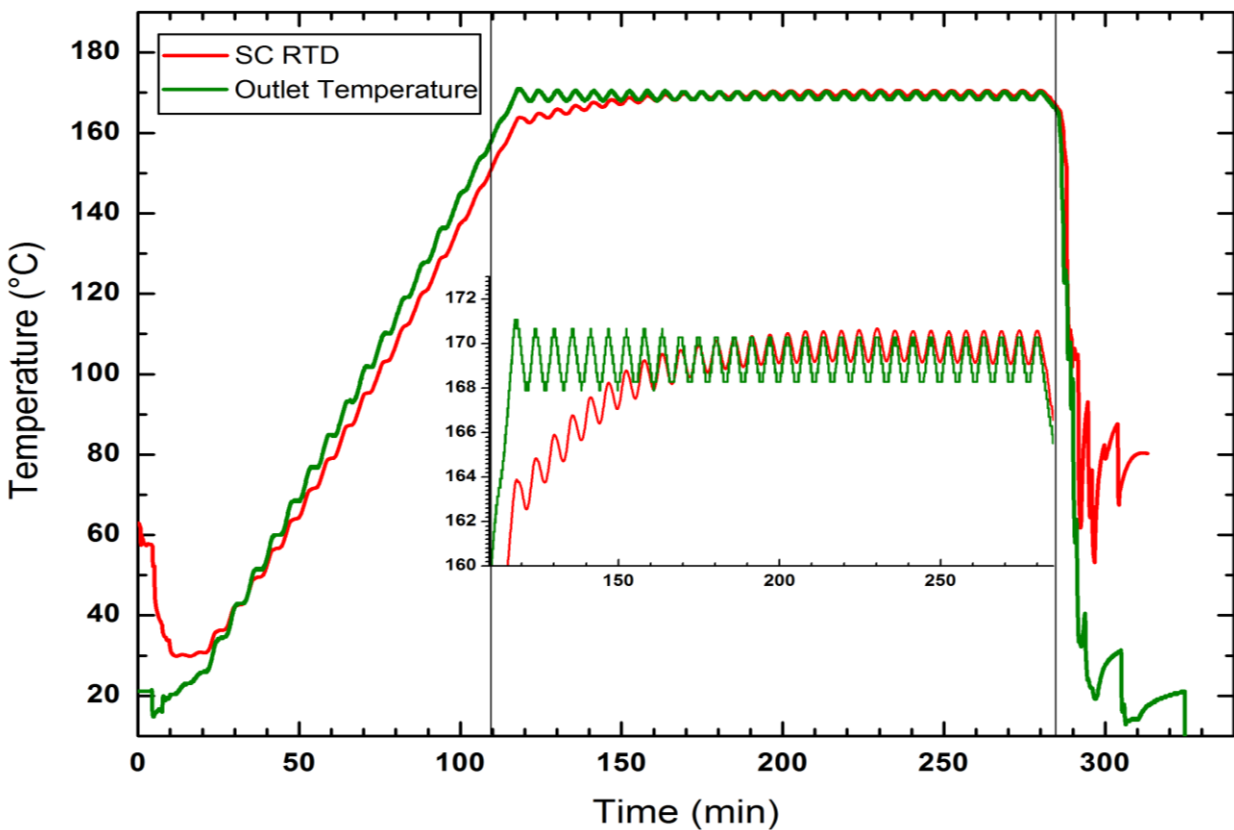


**Figure 10:** Time/temperature data measured (1) by a single SmartChip (with  $10 \times 6 \text{ cm}^2$  PTFE package) placed in the centre of the digester and (2) by the sensor at the liquor circulation loop of the digester, during a kraft cook. The cook took place in a 5L M/K laboratory batch digester, with a cook time of 165 minutes at  $170^\circ\text{C}$ . An inset figure is provided for better illustration of the temperature variability and lag.

Variability can result from temperature gradients during: the rise to temperature, the cooking at constant temperature and the cooling at the end of the cook. Due to the exponential relationship between temperature and reaction rate, it is expected that the majority of the pulp variability will occur during the time-at-cook temperature. For this reason, an inset to better illustrate this period shown in Figure 10. The oscillations seen in time/temperature readings are due to the PID controller cycling the heater to control the temperature profile. The timing of the PID oscillations are aligned in both data sets (the SmartChip temperature profile and the digester sensor outlet temperature profile), however there is a slight lag observed in the temperature profile of the SmartChip, resulting from its thermal mass. The heated digester contents heat up the sensor port as it is a good conductor; however the SmartChip package having a significantly lower thermal conductivity, will be heated at a much slower rate. Hence, this temperature lag results from the time it takes for the package and the sensor to approach thermal equilibrium.

As discussed in section 4.1, the H-factor could be evaluated from the measured time/temperature data. A comparison of the H-factor evaluations was made for the SmartChip and the outlet digester temperature sensor, giving values of 2476 ( $\pm 102$ ) and 2585, respectively - with the accuracy of the liquor circulation loop temperature sensor of the digester being unknown at this stage. The results demonstrated to be good in agreement with one another, with less than 5% variability between them.

The single SmartChip testing in the digester was extended into several cooks with varying cook temperatures and time-at-cook temperatures to provide information on the range of cooking conditions experienced in the independent cooks – details of each cook is presented in Table 1. In cooks 1 to 4, the cooking temperature was kept constant at 170°C and the cooking time was varied between 150 to 190 minutes. The corresponding H-factor for each cook was evaluated using the time/temperature profiles logged by the SmartChip and the kappa number was measured by taking pulp samples from the vicinity of the SmartChip sensor for kappa testing. As expected, an increase in the cooking time would result in an increase in the H-factor and a decrease in the pulp kappa number, as seen in cook 1 through 4. In cooks 2 and 5, the cooking times were kept constant while the cook temperature was increased by 5°C, increasing the H-factor by a factor of 1.5 and decreasing the kappa number by 25%. The significant increase in H-factor and decrease in kappa number results from the exponential relationship between

temperature and pulping reaction rate, as explained previously. The correlation between the H-factor and kappa number for all the cooks are shown in Figure 11.

**Table 1: Specifications and kappa test results for five kraft cooks conducted in a 5L M/K laboratory batch digester with a single SmartChip positioned in the centre, under the cook conditions specified in section 6.1, but varying cook temperature and time-at-cook temperature.**

Cook #	1	2	3	4	5
Maximum cook temperature (°C)	170	170	170	170	175
Time-at-cook temperature (min)	150	170	165	190	170
SmartChip H-factor	2,256	2,589	2,476	3,104	3,906
Average Kappa	21.5	21.0	21.2	19.0	16.8

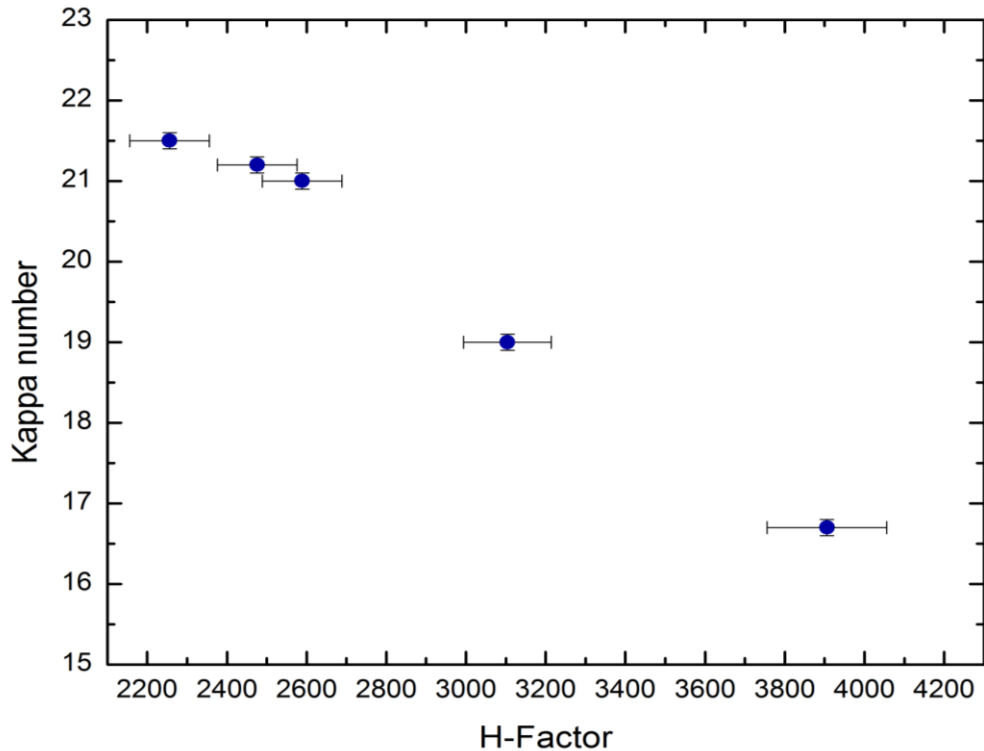


**Figure 11: Correlation between H-factor and Kappa number for the digester cooks given in Table 1**

The key objective of the single SmartChip testing was to ensure that it could withstand the harsh kraft pulping conditions and survive the digester environment. Some problems were faced initially including liquor leakage into the internals of the SmartChip and failure to record the readings during the cook. These difficulties were overcome by some minor design modifications, and eventually the SmartChip was able to successfully record the time/temperature data in the digester for the majority of the kraft cook trials, as already shown in the results of this section.

However, there was the concern of making the SmartChip package smaller and its density closer to that of the wood chips, and so for the subsequent trials, the  $7.5 \times 4 \text{ cm}^2$  PEEK packaging was employed. The new package had two temperature sensors mounted on it, as shown in Figure 8. Another single SmartChip cook trial was conducted with the new SmartChip package under the exact same cooking conditions explained previously with a time-at-cook temperature of 165 minutes. The results of the temperature profiles for the SmartChip temperature sensors and the digester sensor measuring the outlet temperature are presented in Figure 12.

The time/temperature readings for the SmartChip sensors and the digester sensor were in good agreement with one another as shown in Figure 12. Moreover, the temperature lag was reduced significantly, in comparison to the temperature profile given in Figure 10. This was due to the new and smaller package, which was constructed from PEEK, having a slightly higher thermal conductivity (about 2% greater than PTFE) and also the usage of less packaging material, hence increasing the rate of heating. Finally, the orientation of the sensors and the way they were mounted was slightly modified to have less contact with the package. Hence, these design modifications led to a very significant decrease in the temperature lag of the SmartChip readings as shown in Figure 12. The next section of this chapter looks into evaluating delignification diversity within the digesters through the use of multiple SmartChips.

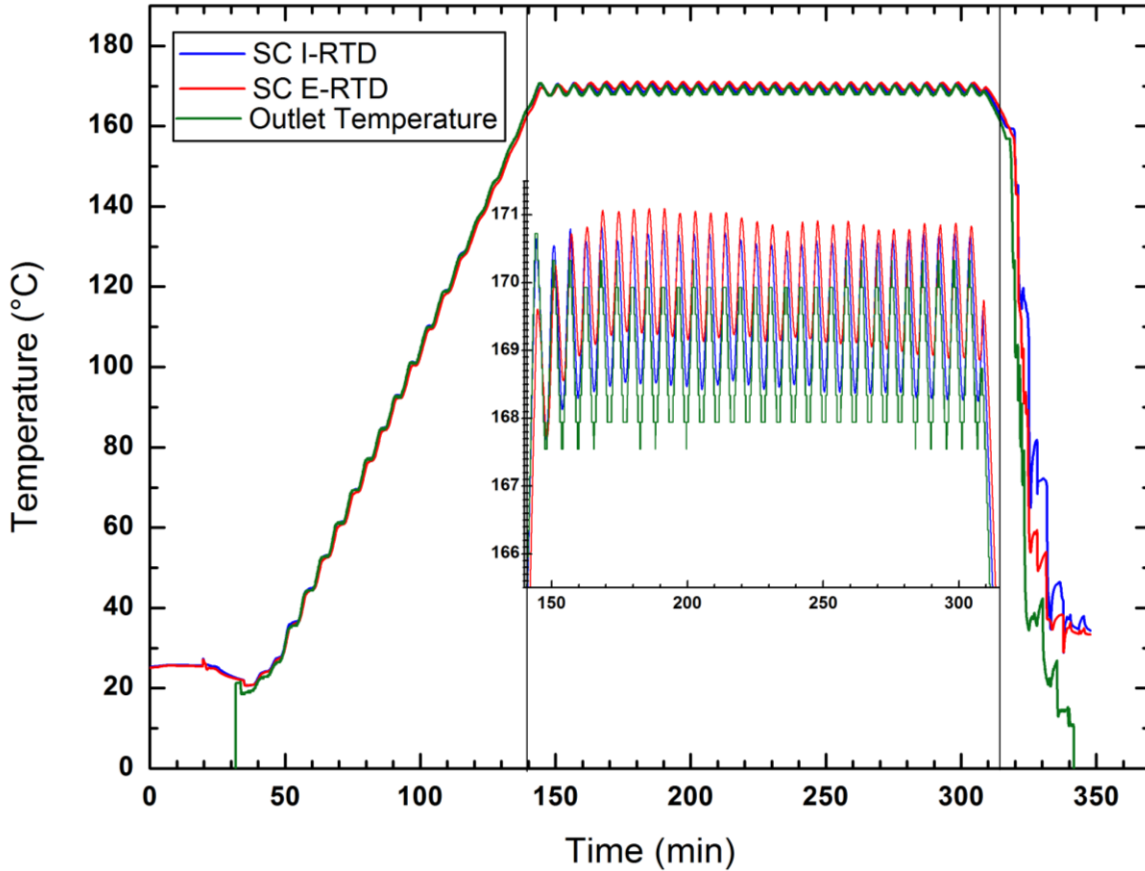


**Figure 12: Time/temperature data measured (1) by a single SmartChip (with  $7.5 \times 4 \text{ cm}^2$  PEEK package and its two sensors I-RTD and E-RTD ), placed in the centre of the digester and (2) by the digester temperature sensor at the outlet, during a kraft cook. The 5L M/K laboratory batch digester was employed; with the cook time of 165 minutes at  $170^\circ\text{C}$ . An inset figure for the time-at-cook temperature is provided for better illustration of the temperature variability.**

## 7.2 SmartChip Trials in 5L M/K Batch Digester

The experimental work in this section involves the deployment of several SmartChips in a single cook to determine the time/temperature history that the wood chips experience in different parts of the digester. The aim of this experimental work was to measure the temperature distribution in the digester during the kraft cook using the SmartChips and then validate the heat transfer model proposed in Chapter 4 based on these experimental results.

### 7.2.1 Experimental Results

Two SmartChips (both with the  $7.5 \times 4 \text{ cm}^2$  PEEK packaging) were positioned at the top and bottom of the vertical centreline of the digester in the 5L M/K laboratory batch digester, under the conditions specified in section 6.2.1. The SmartChip SC001 was placed at the top of the digester and SC002 at the bottom, about 20 cm apart; with both SmartChips aligned in a way that the E-RTD sensor was below the I-RTD sensor. Figure 13 shows the temperature profiles recorded by the SmartChip sensors. The I-RTD sensor on SC001 was placed in the uppermost region of the digester, and so there were times during the cook where it was not completely swathed in liquor, resulting in irrelevant temperature readings taken by this sensor. Also, this sensor failed to take measurements halfway during its transit through the digester. For this reason, the temperature readings of the I-RTD sensor on SC001 are not included in Figure .

The oscillations seen in the SmartChip temperature readings are due to the PID controller cycling the heater to control the temperature profile. With the digester being heated indirectly, heated liquor enters through the top of the digester and leaves through the bottom. An inset is given in Figure 13 to better illustrate the temperature variability during the cook phase. However, it is seen that the temperature variation between the two SmartChips was within the error range of the SmartChip temperature readings (after calibration, the absolute accuracy was reported to be  $\pm 0.52^\circ\text{C}$ , as explained in section 5.2 and Appendix C). Hence, it was difficult to state with confidence whether the temperature variation between the two SmartChips was significant.

The SmartChip timekeeping is handled by an internal oscillator with a calibrated temporal error of  $\pm 20 \text{ ms}$  per interval (4 second intervals) [52]. At the beginning of the cook, both SmartChips are initialized and then powered up simultaneously to synchronize the internal clocks — a small inset is given in Figure 13 showing the synchronization of both sensors at the beginning of the cook. However by the time the SmartChip reaches the cook temperature, the maximum accumulated temporal error is  $\pm 30 \text{ s}$  and by the end of the cook, the accumulation in the interval error reaches a minute and a half — another inset is given in Figure 13.

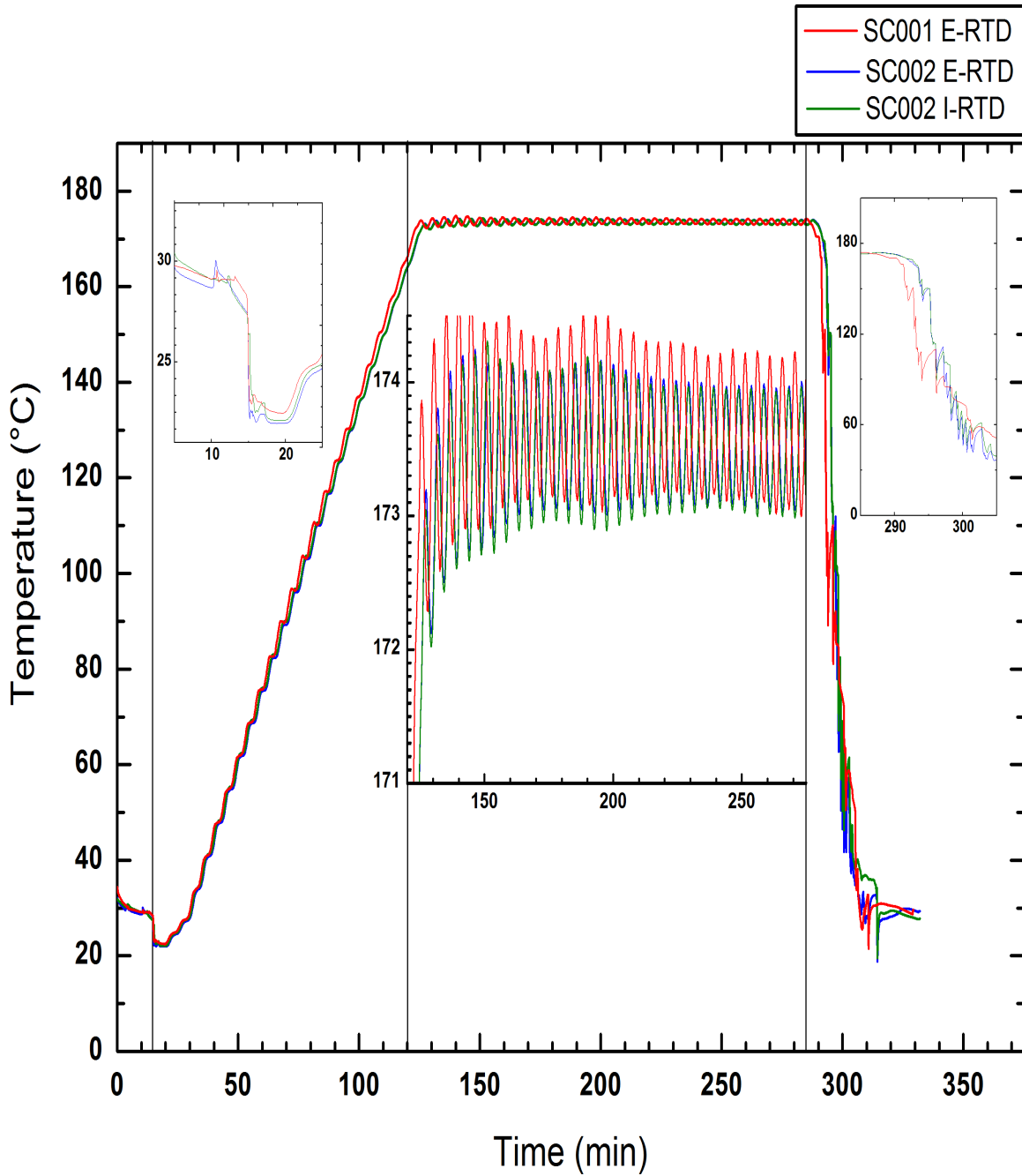


**Figure 13: Time/temperature data measured by two SmartChips, SC001 placed at the top and SC002 placed at the bottom – approximately 20 cm apart. Wood chips were cooked in a 5L M/K laboratory batch digester, with the cook time of 165 minutes at 170°C. Inset figures are provided for better illustration of temperature variability and lag.**

A more detailed investigation into the temperature oscillations and lag during the time-at-temperature period has been conducted. Figure 14 illustrates the initial temperature oscillation for both SmartChips, during the time-at-temperature period. With regards to the amplitude of oscillations, it can be seen that there is a decrease in the magnitude of amplitude when travelling down along the height of the digester — 40% decrease in amplitude between the E-RTD sensors on SC001 and SC002. Whereas, the temperature profiles of both sensors (I-RTD and E-RTD) on SC002 align closely as they are positioned so close to one another. Moreover, there is a slight temperature lag of 2 minutes  $\pm$ 30s in the profiles of the sensors on SC002, which is positioned lower down the digester compared with SC001.

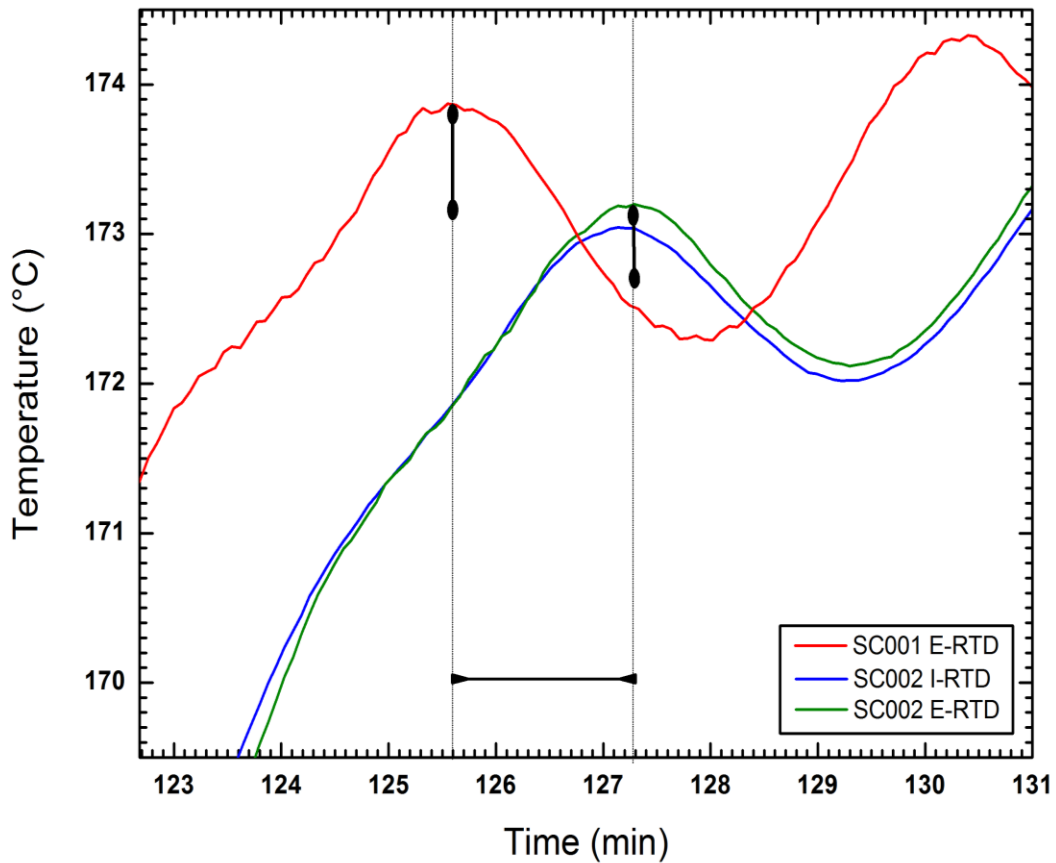


**Figure 14: Magnification of the initial temperature oscillation for both SmartChips (SC001 placed at the top and SC002 placed at the bottom) once the cook just reaches the maximum temperature. This is to show the temperature lag and decrease in amplitude, moving down the digester length.**

As explained earlier, the oscillations in the SmartChip temperature readings result from the PID controller. Figure 14 compared the initial temperature oscillation for both SmartChips, showing the temperature lag between the two SmartChips, while traveling down the digester length. This study is exceeded by evaluating the times at which the temperature profile of each SmartChip reaches its peak and Figure 15 shows the difference in time at which the temperature peaks for SC001 and SC002. As it can be seen, SC002 always peaks at a later time, in the range of 1.5 to 3 minutes, with an increasing trend in its lag as the cook progresses. However, it may be that this increase in the lag results from the time interval error which worsens as the cook progresses over time.

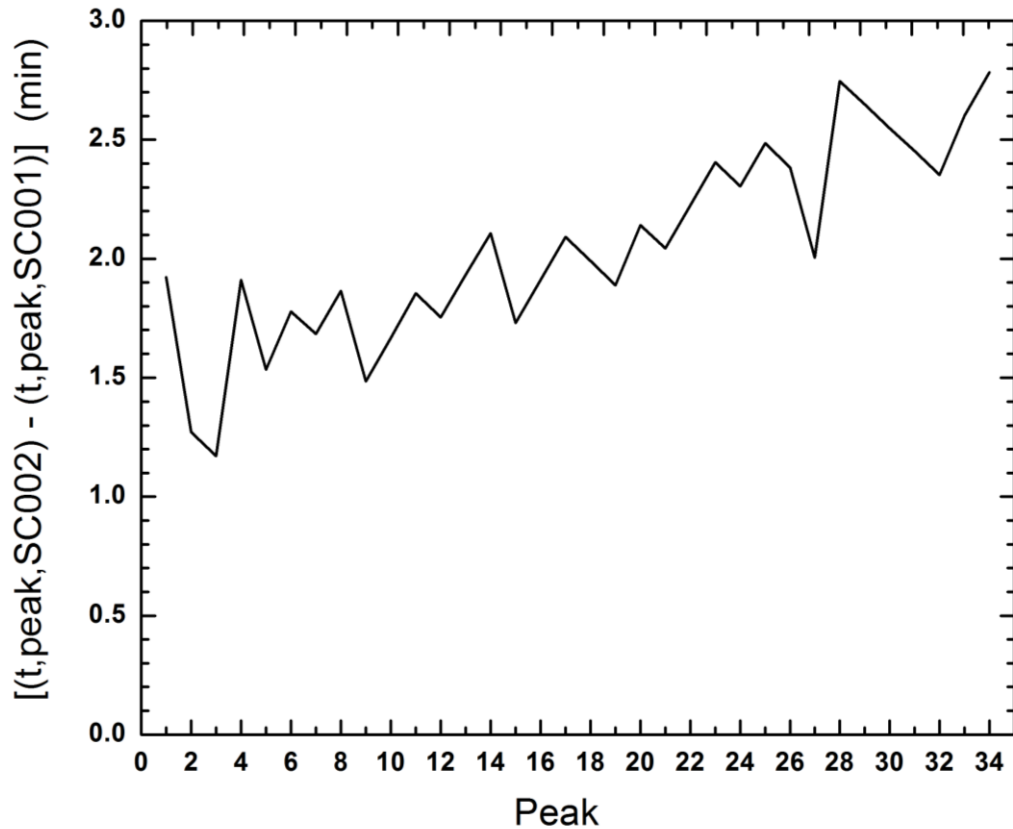


**Figure 15: The difference in the time at which the E-RTD sensor on each SmartChip reaches the peak temperature, i.e., the y-axis is  $[(t_{PEAK,SC002}) - (t_{PEAK,SC001})]$  and the x-axis is the peak number during the time-at-cook temperature— there are 34 peaks in total during the time-at-cook temperature for this case.**

## 7.2.2 Model Validation

A mathematical model describing the heat transfer mechanisms occurring within the digester during the kraft cook was developed in Chapter 4. To validate this model, it was first required to solve the model and then compare the model predictions with the experimental results in Section 7.2.1.

The dimensionless one-equation model describing the temperature variability along the digester was given in Equation (26) in Section 4.4. Primarily, it is required to verify that the single governing equation approach is applicable to the experiment under study, which only applies if the thermal conductivities of the digester constituents do not differ widely. The thermal conductivity of the pine wood was evaluated based on Equation (25) and the thermal conductivity of the cooking liquor was assumed to be the same as that of water, and the results of these calculations showed that these values were of the same order of magnitude hence confirming the validity of thermal equilibrium and the single-equation approach. The values of  $\lambda$  and  $\varepsilon$  in Equation (26) could then be evaluated, provided that the digester dimensions, the flow of liquor along the digester and the thermo-physical properties of the wood are known. Solving for the values of  $\lambda$  and  $\varepsilon$  gave solutions in the order 1 and  $10^{-4}$  respectively. Hence, with the value of  $\varepsilon$  being so small, it could be predicted from this model that the heat transfer in the digester was by pure advection.

Based on the exponential relationship between temperature and reaction rate, it is expected that temperature variability during the time-at-cook temperature would contribute most to pulping heterogeneity. For simplification purposes, this work will only concentrate on understanding the heat transfer within the digester and solving for Equation (26) during this period of the cook - with the boundary conditions given accordingly in Equations (27) and (28). At the top of the digester, the dimensionless temperature is equivalent to one, however there are oscillations accompanying it due to the PID controller cycling the heater to control the temperature profile of the digester, bringing about the  $asin(\omega t)$ , with  $a$  being the amplitude of the oscillations and  $\omega$  being the angular frequency. As explained previously, by the time the liquor reaches the bottom of the digester, it has minimum temperature and so the zero heat flux condition is used.

$$x^* = 0 \qquad T^* = 1 + asin(\omega t) \qquad (27)$$

$$x^* = 1 \quad \frac{\partial T^*}{\partial x^*} = 0 \quad (28)$$

The temperature profile of the digester contents is expected to vary sinusoidal with time- being dependant upon the position along the digester, as shown in Equation (29). Based on Euler's formula, the trigonometric function in Equation (29) is converted into a complex exponential function as shown in Equation (30). The temperature profile of the digester contents, that is Equation (30), is differentiated with respect to position and time and substituted into Equation (26) to give Equation (31), which is further simplified to give Equation (32).

$$T^* = 1 + a \sin(\omega t) \cdot g(x) \quad (29)$$

$$T^* = 1 - a i e^{i \omega t} g(x) \quad (30)$$

$$a \omega e^{i \omega t} g(x) - \lambda a i e^{i \omega t} \frac{\partial g}{\partial x^*} = -\varepsilon a i e^{i \omega t} \frac{\partial^2 g}{\partial x^{*2}} \quad (31)$$

$$\text{with } \frac{\partial T^*}{\partial t^*} = a \omega e^{i \omega t} g(x)$$

$$\frac{\partial T^*}{\partial x^*} = -a i e^{i \omega t} \frac{\partial g}{\partial x^*}$$

$$\frac{\partial^2 T^*}{\partial x^{*2}} = -a i e^{i \omega t} \frac{\partial^2 g}{\partial x^{*2}}$$

$$i \omega g(x) + \lambda \frac{\partial g}{\partial x^*} = \varepsilon \frac{\partial^2 g}{\partial x^{*2}} \quad (32)$$

This problem can be approximated as a single perturbation, since the value of  $\varepsilon$  is very small in the order of magnitude of  $10^{-4}$ , but cannot be approximated by setting it to zero. In order to solve the singularly perturbed partial differential equation, the method of matched asymptotic expansion is employed to find an approximation to the answer of the problem. Hence, the domain is divided into two sub-domains resulting in an inner solution and an outer solution to the problem.

Formally, we seek a solution to the problem with an expansion of the form:

$$g(x) = g_0(x) + g_i(x; \varepsilon) \quad (33)$$

where  $g_0$  represents the outer solution and  $g_i$  represents the inner solution. In the outer solution, the problem is treated as a regular perturbation by setting the value of  $\varepsilon$  to zero, as given in Equation (34). In the inner solution, the perturbation term cannot be neglected, as given in Equation (35).

$$\text{Outer Solution: } \omega g_0(x) = \lambda i \frac{\partial g_0}{\partial x^*} \quad (34)$$

$$\text{Inner Solution: } i\omega g_i(x) - \lambda \frac{\partial g_i}{\partial x^*} = -\varepsilon \frac{\partial^2 g_i}{\partial x^{*2}} \quad (35)$$

These relationships can be integrated directly to give:

$$g_0(x) = \exp\left(\frac{-i\omega x}{\lambda}\right) \quad (36)$$

$$g_i(x) = \frac{-i\omega}{\lambda^2} \exp\left(\frac{-i\omega}{\lambda}\right) \cdot \exp\left(\frac{-\lambda(1-x)}{\varepsilon}\right) \quad (37)$$

$$g(x) = \exp\left(\frac{-i\omega x}{\lambda}\right) - \frac{i\omega}{\lambda^2} \exp\left(\frac{-i\omega}{\lambda}\right) \cdot \exp\left(\frac{-\lambda(1-x)}{\varepsilon}\right) \quad (38)$$

With this and Equation (29), the temperature field is given by this equation:

$$T(x, t) = 1 + a \left[ \underbrace{\sin\left(\omega\left(t - \frac{x}{\lambda}\right)\right)}_{\text{I}} - \underbrace{\frac{\omega}{\lambda^2} \cdot \exp\left(-\frac{\lambda}{\varepsilon}(1-x)\right) \cdot \cos\left(\omega\left(t - \frac{1}{\lambda}\right)\right)}_{\text{II}} \right] \quad (39)$$

The temperature of the digester contents as a function of the axial position along the digester and time during the kraft cook is evaluated based on equation (39). The first part of this equation (I) represents the transport of heat along the digester by fluid motion, also known as heat advection. The temperature of the digester contents varies in a sinusoidal manner with time, and as a result of the advective heat transfer, the time at which the sine waves peak is shifted to the left while moving down the digester. The second part of this equation (II) represents the transfer of heat to the wood chips and with the value of  $\varepsilon$  being very small of order  $10^{-4}$ , this part of the equation

could be considered negligible. Overall, the mathematical model could be employed to describe the heat transfer mechanisms within the digester, with the results revealing that thermal energy required for heating of wood chips is nearly insignificant, and that the heat transfer through the digester contents is by pure advection.

Model validation is conducted by the comparison of these predictions with the experimental results from the SmartChip readings in Section 7.2.1. As shown in Figure , the difference in time at which the temperature peaks for the two SmartChips is in the range of 1.5 to 3 minutes. With a crude calculation of the liquor velocity through the digester shell, it is evaluated that it would take approximately  $1.7 \pm 0.2$  minutes to travel the distance between the two SmartChips, based on the prediction that heat transfer along the digester is by pure advection. This value is in agreement with the experimental results taken from the SmartChip readings, hence verifying the model prediction that the heat transfer within the digester is solely by advection. However, it is important to note that the experimental results show an increasing trend in the lag of up to about 3 minutes by the end of the cook, which is not due to any physical reasoning but rather predominantly associated with the time interval error which worsens as the cook progresses over time.

### **7.3 SmartChip Trials in 20L Batch Digester**

Digester variability studies within a larger 20L batch digester were conducted based on the experimental specifications in Section 6.2.2. Two trials were conducted and the wood chips were cooked under the same conditions explained previously, but varying time-at-cook temperatures: 51 and 106 min respectively. Two SmartChips were positioned ( $\approx 35$  cm apart) at the top and bottom of the digester and inverted for the two cooks, i.e., SC001 was placed at the bottom in cook 1 and at the top during cook 2. Figure 16 shows the temperature profiles recorded by the SmartChip sensors for the two cooks.

The better optimized PID parameters of the 20L controller digester eliminated the control oscillations seen in the 5L M/K digester. A comparison of the temperature lag along the length of the digester for both runs shows that the top SmartChip reached the cook temperature faster than the bottom SmartChip. Inverting the SmartChip positions in the two cooks and observing the same results, further verified this hypothesis.

The temperature gradient in the axial direction of the digester during the time-at-temperature period is shown by an inset in Figure 16. The temperature variation in the digester is very small, within the relative error range of the temperature sensors on the SmartChips, indicating that the temperature in the digester is already well-controlled. More precise measurements will be needed in order to determine the temperature variability within these small scale digesters.

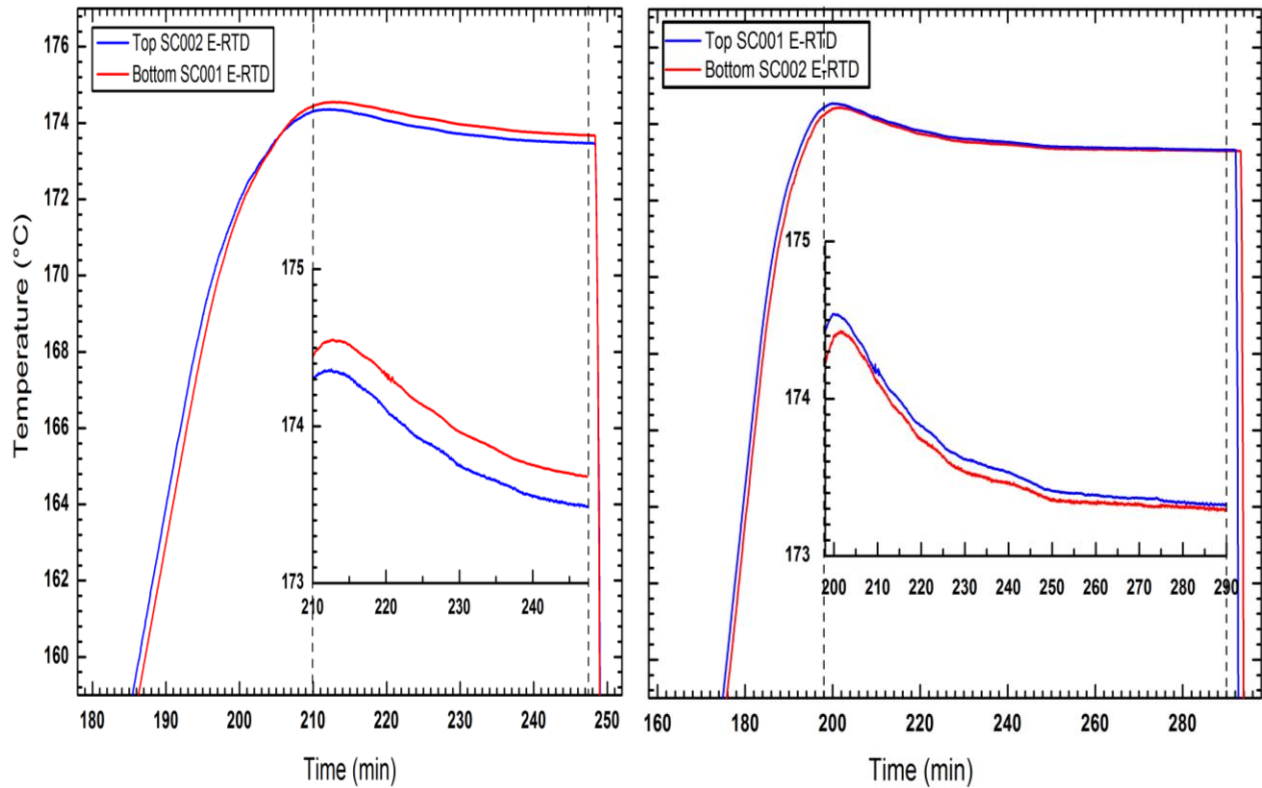


**Figure 16: Time/temperature data measured by the SmartChips SC001 and SC002 in the 20L batch digester during a kraft cook. For the first trial (left figure), the time-at-cook temperature was 51 minutes, SC001 at the bottom and SC002 at the top of the digester. In the second trial (right figure), the time-at-cook temperature was 106 minutes, with the SmartChip positions inverted. An inset figure is given to better illustrate the temperature variability and lag.**

To establish a correlation between the temperature gradients and pulp variability, pulp samples were taken from the vicinity of the SmartChip sensors for kappa testing. These samples were taken from the vicinity of SC001 and SC002 sensors and also a small portion was taken from the space in between them. A scatter plot of the kappa test results for three consecutive cook trials in the 20L batch digester with varying target H-factors are presented in Figure 17. In all the cooks, the bottom of the digester always had the lowest kappa, whereas no consistent kappa pattern was observed for the pulp at the top and middle of the digester. The results did not show any significant correlation between the temperature gradient and pulp variability, however, this does not suggest that it is not important to control temperature; but instead, validates that it is already well-controlled within these small-scale digesters.

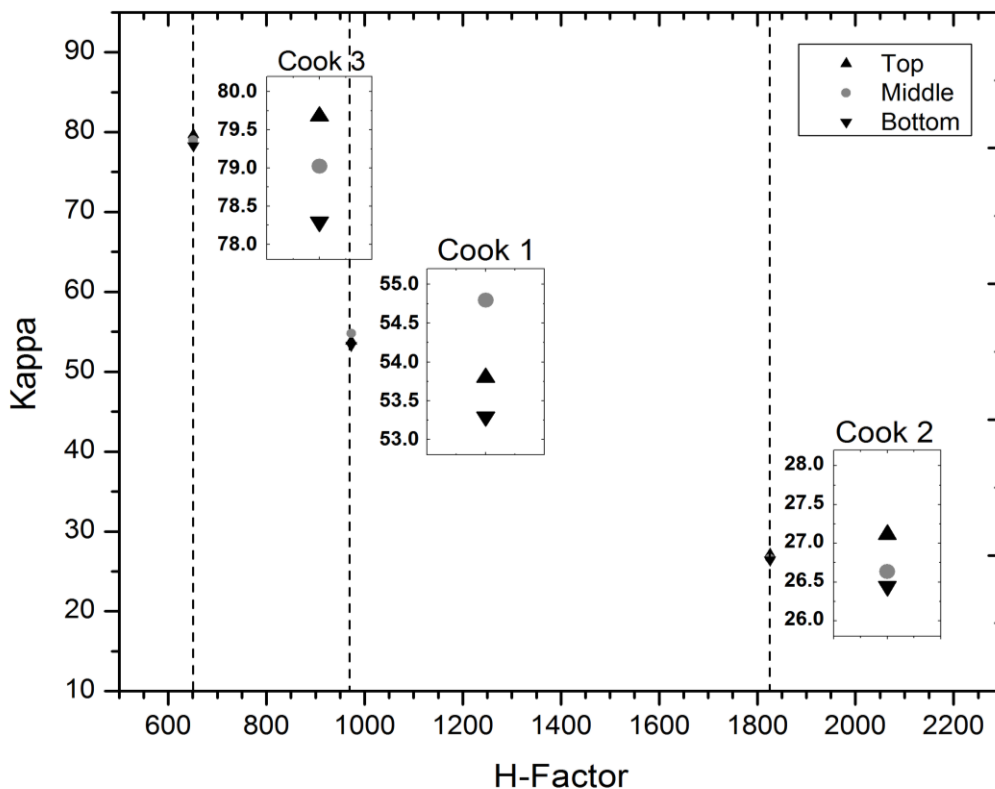


**Figure 17: Kappa test results from pulp samples taken from the top, bottom and middle of the digester, for three cooks in the 20L batch digester. For each trial, the wood chips are cooked for varying time-at-cook temperatures resulting in varying target H-factors.**

## 8 Closing Remarks

### 8.1 Summary and Conclusions

A novel method to measure variability within digesters during a kraft cook has been developed in this research: the “SmartChip.” This device is designed, developed and constructed to measure and record the temperature directly within the digester during the cook. Primarily, a single SmartChip was tested in a laboratory scale batch digester to ensure that it could survive the harsh kraft pulping environment. Having accomplished this objective through numerous cooking trials and various design modifications, the subsequent step involved the deployment of multiple SmartChips in a single cook to obtain insight on the temperature variability and the heat transfer mechanisms occurring within the digester.

Prior to the experimental work, a theoretical model describing the heat transfer mechanisms inside the digester was developed. This model showed that the thermal energy required for heating of wood chips was very small, and that the heat transfer through the digester contents was purely advective. The model was then validated by comparing the predictions with the experimental results. The experimental work involved positioning two SmartChips at the top and bottom of a 5L M/K laboratory batch digester and comparing their temperature profiles during a kraft cook. The results showed a temperature lag of  $2 \text{ min} \pm 30\text{s}$  between the two SmartChip readings. By evaluating the velocity of the liquor through the porous medium and the distance between the two SmartChips, it could be deduced that this time lag corresponded to the time taken for the liquor to travel the distance along the digester between the two SmartChips. Hence, this verified the model prediction of advective heat transfer through the digester.

With nonuniformity becoming more of an issue with the increasing size of digesters, SmartChip testing was extended to a larger, 20L batch digester. With regards to the temperature lag between the two SmartChips, a similar behavior to the previous case was observed. Moreover, for both digesters, temperature variations between the two SmartChips fell within the error range of the sensors, indicating that there was little variability and that temperature was already well-controlled within these small scale digesters – as anticipated. Based on these observations, it could be further concluded that the SmartChip can withstand the harsh conditions of the kraft

process and is sufficiently robust for use in digesters. Moreover, its further development is warranted at the industrial scale, where temperature fluctuations are more noticeable.

## **8.2 Recommendations and Future Work**

This thesis has established a foundation upon which future work could be built upon. This work could take several forms, including extending the use of the prototype SmartChip into industrial digesters, as well as the development of a smaller, IC (Integrated Circuit) SmartChip, which better mimics the behaviour of the actual wood chips.

Multiple SmartChips deployed in the laboratory batch digesters showed little variability due to the small size of digesters. For future work, these experiments could be extended into the industrial scale, both batch and continuous digesters, where temperature gradients are more noticeable and nonuniformity is more of a concern. In such cases, it is required that a static pressure sensor be included on the prototype SmartChip, which would allow its vertical position to be tracked. Hence, multiple SmartChips deployed in a single cook within an industrial digester would determine the time/temperature history that the wood chips experience, along various elevations inside the digester, during the kraft cook.

Moreover, in the deployment of SmartChips in continuous digesters, an important issue to address is the complications associated with the SmartChip retrieval. It is anticipated that once discharged into the continuous system, the SmartChip would be retrieved from the bunker. Also, with knowledge of the flow rate of the contents within the digester, the approximate time of retrieval could also be predicted. With the pulping system designed in a way to eject any undigested material, SmartChip retrieval is warranted. However, the survival of the SmartChip during its journey through the industrial digesters and the rate of attrition associated with it, are still questionable and require further experimentation.

Another dimension to this project would be the development of an IC SmartChip, which more closely mimics the size, shape and density of a typical wood chip. Some study has already been committed into its development. The IC SmartChip is designed to be equipped with an additional sensor: a conductivity sensor for measuring the alkali content variability within the digester during the kraft cook. Moreover, it has a modular platform to enable the addition of

supplementary sensors. The ultimate objective would be the development of SmartChips that experience the exact same conditions as the wood chips and measure the essential parameters for evaluating exactly what is going on within the digesters as well as evaluating extent of nonuniformity within them. Moreover, there have been plenty of disputes regarding the online collection of data, as opposed to downloading upon retrieval, but with the large metal digesters being in the picture, this issue is still under extensive argument.

## References

- [1] Hamilton, R. P. (1961). "Measurement of Kamyr Continuous Kraft Digester Cooking Cycle Using Radioactive Tracers", *Tappi*, 44 (9), 647-655.
- [2] Vlaev, D. S. and Bennington C. P. J. (2005). "Flow Uniformity in a Model Digester Measured with Electrical Resistance Tomography", *The Canadian Journal of Chemical Engineering*, 83 (1), 42-47.
- [3] Thompson, S. L. And Gustafson R. R. (2000). "Effects of Kappa Variability on Pulp Properties", *Tappi*, 83 (1), 157-163.
- [4] Market Pulp Association (2007). "Overview of the Wood Pulp Industry", Retrieved January 25, 2010, from [http://www.pppc.org/en/2\\_0/2\\_1.html](http://www.pppc.org/en/2_0/2_1.html).
- [5] Horner, R. (1996). "Pulp and Paper Industry Advisory Committee Report", *BC Competition Council*.
- [6] Smook, G. A., (1992). "Handbook for Pulp and Paper Technologists", Vancouver: Angus Wilde Publications, 36-82.
- [7] MacLeod, J. M., McPhee, F. J., Kingsland, K. A., Tristram, R. W., O'Hagan, T. J., Kowalska, R. E. and Thomas B. C. (1995). "Pulp Strength Delivery along Complete Kraft Mill Fibre Lines", *Tappi*, 78 (8), 153-160.
- [8] Aguiar, H. C. and Filho, R. M. (2001). "Neural Network and Hybrid Model: A Discussion about Different Modeling Techniques to Predict Pulping Degree with Industrial Data", *Chemical Engineering Science*, 56 (2): 565-570.
- [9] Carvalho, K. H. A., Silva, M. L. and Soares, N. S. (2009). "Competitiveness of the Brazilian Wood Pulp in the International Market", *Cerne*, 15 (4): 383-390.
- [10] Tikka, P. O., MacLeod, J. M. and Kovasin K. K. (1991). "Chemical and Physical Performance of Kraft Cooking: the Impact of Process Alternatives", *Tappi*, 74 (1): 137.143.

- [11] RISI, (2009) “World Pulp Annual Historical Data – Excerpt,” Table 4 – World Production.
- [12] Tichy J. and Procter A. R. (1981). “Measurement and Significance of Lignin Content Uniformity in Unbleached Kraft Pulps”, *Svensk-Papperstidning*, 84 (15): R116-R122.
- [13] Earl, P. F. and Pryke, D. C. (2005). “Softwood Bleaching Practices in Canada: Analysis of the 2003 PAPTAC Bleaching Committee 'Best Practices' Survey”, *Preprints 91<sup>st</sup> Annual Meeting PAPTAC*, B281-B289.
- [14] Grace T. M. and Malcom E. W. (1983). “Pulp and Paper Manufacture - Volume 5: Alkaline Pulping”, Joint Textbook Committee of the Pulp and Paper Industry, Atlanta: Tappi.
- [15] Pageau G. L. And Davies D. (2000). “Analysis of Fibreline Log Sheet Survey”, *Pulp and Paper Canada*, 101 (11): 39-43.
- [16] MacLeod, J. M. (1990). “Basket Cases: Kraft Pulp Strength Variability within a Batch Digester”, *Tappi*, 73 (10): 185-190.
- [17] Tikka, P. O. and Kovasin K. K. (1990). “Displacement vs. Conventional Batch Kraft Pulping: Delignification Patterns and Pulp Strength Delivery”, *Paperi Ja Puu – Paper and Timber*, 72 (8): 773-779.
- [18] Tikka, P. O. (1992). “Conditions to Extend Kraft Cooking Successfully”, *Tappi Pulping Conference*, 669-706.
- [19] Malkov, S. ,Tikka P. and Gullichsen J. , Nuopponen M. and Vuorinen T. (2003). “Towards Complete Impregnation of Wood Chips with Aqueous Solutions” *Paperi Ja Puu*, 85 (8): 460-466.
- [20] Gustafson, R. R., Jimenez G., McKean W. T. and Chian D. S. (1989). “The Role of Penetration and Diffusion in Nonuniform Pulping of Softwood Chips”, *Tappi*, 72 (8): 163-167.
- [21] Akhtaruzzaman, A. F. M. and Virkola, N. E. (1979). “Influence of Chip Dimensions in Kraft Pulping - Part III: Effect on Delignification and a Mathematical Model for Predicting the Pulping Parameters” *Paperi Ja Puu*, Vol. 61 (11): 737-758.

- [22] Twaddle, A. (1997). Oversize Chip Formation and Relationship to Chip Length. *Tappi Pulping Conference*, 307-315.
- [23] Farrington, A. (1980). “Wood and Digester Factors Affecting Kraft Pulp Quality and Uniformity”, *Appita*, 34 (1): 40-46.
- [24] Luu, N. H. and Shariff A. (2003). “Defining Optimum Chip Size for a Market Softwood Kraft Mill Using an Empirical Model Developed from Layered Cooking of Chips”, *PAPTAC 87<sup>th</sup> Annual Meeting*, B13-B19.
- [25] Vroom, K. E. (1957). “The H-Factor: A Means of Expressing Cooking Times and Temperature as a Single Variable”, *Pulp and Paper Canada*, 58 (3): 228-231.
- [26] Rayal, G., Gustafson, R., Arvela, M. and Rantamaki, J. (2005). “On the Relationship between Pulping Temperature and Kraft Pulp Kappa Uniformity at the Single Fibre Level”, *Paperi Jaa Puu - Paper and Timber*, 87 (5): 329-332.
- [27] Qiao, M. and Gustafson, R. (2007). “Influence of Fibre-Scale Heterogeneity on Softwood Kraft Pulp Uniformity”, *Journal of Pulp and Paper Science*, 33(4):227-232.
- [28] Robinson, J. K., Gustafson, R. R., Callis, J. B. and Bruckner, C. (2002). “Measurement of Kappa Number Variability on the Fibre Level”, *Tappi*, 1 (10): 3-8.
- [29] Lee, Q. F. and Bennington C. P. J. (2007). “Spatial Distribution of Kappa Number in Batch Digesters: 2D Model”, *Journal of Pulp and Paper Science*, 33 (4): 206-216.
- [30] McDonald, S. (2002). “Digester Operations – Batch”, Kraft Pulping Short Course, Norcross: Metso Paper .
- [31] Wisnewski, P. A. and Doyle, F. J. (1997). “Fundamental Continuous-Pulp Digester Model for Simulation and Control”, *AIChE Journal*, 43 (12): 3175-3192.
- [32] Fan, Y. (2005). “Numerical Investigation of Continuous Industrial Digesters”, Vancouver: University of British Columbia, Mechanical Engineering, Thesis.

- [33] Johansson, B., Mjöberg, J., Sandström, P. and Teder, A. (1984). "A Modified Continuous Kraft Pulping - now a reality", *Svensk Papperstidn*, 87 (10) 30-35.
- [34] Tran, A. V., (2005). "Characterisation of a Conventional Kamyr Continuous Digester producing Hardwood Kraft Pulp", *Appita*, 58 (1): 22-27.
- [35] Marcoccia, B., Prough J. R., Engstorm J. And Gullichsen J. (2000), "Continuous Cooking Applications." Papermaking Science and Technology 6. *Chemical Pulping*, Gullichsen J. And Fogelholm C. J. (eds), Tappi and Finnish Paper Engineerings' Associations Book, A513-A570..
- [36] Kleppe, P. J. (1970). "Kraft Pulping", *Tappi*, 53 (1): 35-48.
- [37] Shomaly, Y. H., (1990). "Uniformity of Kraft Pulping", Chemical Engineering, McGill University, Pulp and Paper Research Institute of Canada, MEng Report.
- [38] Sherban, C. (2003). "Improving Pulp Quality and Uniformity in Indirectly Heated Batch Digesters", *Tappi Fall Tech. Conference*, Chicago, IL.
- [39] Pulp and Paper Research Institute of Canada, "Chemical Pulping Towards the Year 2000". Pointe Claire, QC.
- [40] Lee, Q. F. and Bennington, C. P. J. (2007). "Measuring Flow Velocity and Uniformity in a Model Batch Digester Using Electrical Resistance Tomography", *The Canadian Journal of Chemical Engineering*, 85 (2): 55-64.
- [41] Kubulnieks, E., Lundqvist, S. and Pettersson, T. (1987). "The STFI OPTI-Kappa Analyzer: Applications and Accuracy.", *Tappi*, 70 (11): 38-41.
- [42] Tikka, P. and Piironen, P., (1987). "Cooking Liquor Analyzer: A New Tool for Controlling a Continuous Digester", *Pulp and Paper Canada*, 88 (10): T387-T392.
- [43] Laitinen, M., Kemppainen, A. and Backman, M. E. (1999). "Midpoint Kappa Measurement - New Possibilities in Digester Control", *Tappi Pulping Conference Proceeding*, 1217-1223.

- [44] Andrews, P. and Pageau, G. (2006). “Kappa Variability within the Howe Sound Pulp and Paper Continuous Digester”, Port Mellon: Howe Sound Pulp and Paper.
- [45] Hatton, J. V. (1973). “*Development of Yield Prediction Equations in Kraft Pulping*”, *Tappi*, 56 (7): 97-100.
- [46] Kocaefe, D., Younsi, R., Chaudry, B. and Kocaefe, Y., (2006). “Modeling of Heat and Mass Transfer during High Temperature Treatment of Aspen”, *Wood Science Technology*, 40 (3): 371-391.
- [47] Nield, D. A. and Bejan, A., (2006). “*Convection in Porous Media*”, New York : Springer, 27-39.
- [48] Truong, H. V. and Zinsmeister, G. E., (1978). “Experimental Study of Heat Transfer in Layered Composites”, *International Journal of Heat and Mass Transfer*, 21 (7): 905-909.
- [49] Fourie, J. G. and Plessis, J. P., (2003). “A Two-Equation Model for Heat Conduction in Porous Media (I: Theory)”, *Transport in Porous Media*, 53 (2): 145-161.
- [50] Mortha, G. F. and Jain, S., (2008). “Modeling Kraft Cooking of Wood Species Mixtures, *International Journal of Chemical Reactor Engineering*, Vol. 6, A18.
- [51] Simpson, W. and Tenwold, A., (1999). “Physical Properties and Moisture Relations of Wood”, *Wood Handbook*, Madison : USA Forest Service, Forest Products Lab, p123.
- [52] Graham, T. C. M., Liu, E., Mohammadi, A. R., Sadeghi, N., Albadvi, E., Mirabbasi, S., Chiao, M., Madden, J. and Bennington, C. P. J. (2010). “Development of a Flow-Following Sensor Package for Application in Chemical Pulp Digesters”, *Pulp and Paper Canada*, 36 (May/June).
- [53] Tappi Test Method T 236 cm-85: Kappa Number of Pulp (1985).

## Appendices

### Appendix A: Pulping Chemical Preparation

Kraft white liquor was prepared with solid crystals of sodium sulphide ( $\text{Na}_2\text{S}$ ) and sodium hydroxide ( $\text{NaOH}$ ). The required amounts of the two constituents were mixed with deionized water for about 5 to 10 minutes, until the solution homogenized. The solution was then left overnight to allow for cooling due to the exothermic nature of the reaction. Batches of only 2.5 litres were made at a time, being sufficient for only two cooks in the 5L M/K batch digester. Leaving the solution out for too long would cause the solid particles to settle to the bottom, forming a non-homogeneous liquor solution, hence only small batches of cooking liquor were made each time.

The amounts of  $\text{Na}_2\text{S}$  and  $\text{NaOH}$  to be employed for the white liquor preparation are dependent on the target effective alkali charge and sulphidity, as shown in Equations (A1) and (A2) respectively.

$$\text{sulphidity} = \frac{\text{Na}_2\text{S}}{\text{Na}_2\text{S} + \text{NaOH}} \quad (\text{A1})$$

$$\text{EA} = \text{NaOH} + \frac{1}{2}\text{Na}_2\text{S} \quad (\text{A2})$$

Using the above equations, the amounts of  $\text{Na}_2\text{S}$  and  $\text{NaOH}$  (expressed in equivalents of  $\text{Na}_2\text{O}$ ) could be solved – as shown in Equations (A3) and (A4) respectively, where  $z$  is the EA charge and  $y$  is the sulphidity. The amounts of each component are expressed in equivalents of  $\text{Na}_2\text{O}$ ; this compound is not present in the liquor but the expression is by convention.

$$\text{Na}_2\text{S (as Na}_2\text{O)} = \frac{2zy}{2-y} \quad (\text{A3})$$

$$\text{NaOH (as Na}_2\text{O)} = \frac{2z - \text{Na}_2\text{S}}{2} \quad (\text{A4})$$

It is then required to convert the masses from the  $\text{Na}_2\text{O}$  equivalent into the actual amounts. The molecular weights of  $\text{Na}_2\text{O}$ ,  $\text{Na}_2\text{S}$  and  $\text{NaOH}$  are 62 g/mol, 78.1 g/mol and 80 g/mol respectively. Moreover, it is required to consider the purity of the solid  $\text{Na}_2\text{S}$  and  $\text{NaOH}$  that is

being used. The final amounts of Na<sub>2</sub>S and NaOH (in g/l) required for white liquor preparation are evaluated based on the Equations (A5) and (A6).

$$Na_2S = \frac{Na_2S \text{ (as } Na_2O)}{\frac{62}{78.1} \times \% \text{ purity}} \quad (\text{A5})$$

$$NaOH = \frac{NaOH \text{ (as } Na_2O)}{\frac{62}{80} \times \% \text{ purity}} \quad (\text{A6})$$

## Appendix B: Kappa Number Determination

The kappa number of the pulp samples was measured according to the TAPPI 236 cm-85 test method. This is done by weighing out to the nearest 0.001 g, the amount of pulp specimen that would consume approximately 50% of the potassium permanganate solution – this value could be attained from the tables in the literature [53]. The pulp sample is then disintegrated with 500 mL of water and mixed with 50 mL  $\pm$  0.1 mL of potassium permanganate (at 0.1*N*) and 25 mL  $\pm$  0.1 mL of sulphuric acid (at 8.0*N*). A stopwatch is immediately started and the contents are mixed for 10 minutes. A constant temperature of 25°C must be maintained, but for times when a temperature bath is not available, the temperature is determined after the reaction has been taking place for 5 minutes and this is assumed to be the average reaction temperature throughout the test. Consequently, a temperature correction factor,  $f_{temp}$  is used as given in Equation (B3). At the end of exactly 10 minutes, the reaction is stopped by adding 10 ml of potassium iodide (at 1.0*N*). Immediately after mixing, the contents are titrated with sodium thiosulphate (at 0.2*N*) and the amount used is recorded. Moreover, prior to the kappa testing using pulp samples, it is required to carry out a blank solution using the exact same method explained, but without the pulp. The kappa number of the pulp sample is then evaluated based on Equation (B1).

$$K = \frac{p \times f \times f_{temp}}{w} \quad (\text{B1})$$

$$p = \frac{(b-a)N}{0.1} \quad (\text{B2})$$

$$f_{temp} = [1 + 0.013(25 - T)] \quad (\text{B3})$$

where:

$K$  = kappa number

$w$  = weight of moisture-free pulp in the specimen, g

$p$  = amount of 0.1*N* permanganate actually consumed by the test specimen, mL

$b$  = amount of thiosulphate consumed in the blank determination, mL

$a$  = amount of thiosulphate consumed by the test specimen, mL

$N$  = normality of the thiosulphate

$F$  = factor for correction to a 50% permanganate consumption, dependant on the value of  $p$  and can be evaluated from given tables [53].

$f_{temp}$  = factor for temperature correction

$T_r$  = actual reaction temperature, °C

## Appendix C: Calibration

The SmartChip temperature sensor is a resistance temperature detector (RTD) mounted in direct thermal contact to the environment in a Wheatstone bridge configuration, as shown in Figure C1. The output voltage of the Wheatstone bridge is proportional to the RTD's resistance and therefore the temperature. The imbalance in the bridge, produced by the change in resistance of the RTD, is measured by the ADC and converted to temperature by the Calendar-Van Dusen equation:  $R_T = R_0(1 + AT + BT^2)$  - with the values of the constants  $A$  and  $B$  specified by the product manual.

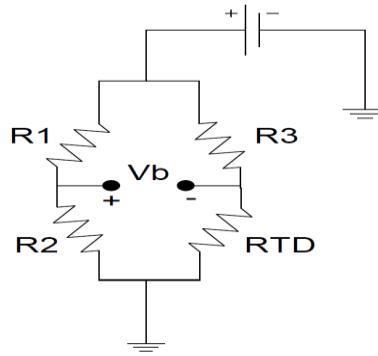


Figure C1: Schematics of the Wheatstone Bridge Temperature Sensor.

The accuracy of the temperature readings taken by the SmartChip is particularly important because the reaction rate is an exponential function of temperature, as explained in section 4.1. The prototype SmartChip needs to both achieve reasonable level of reliability and maintain at least  $\pm 0.5^\circ\text{C}$  absolute accuracy over the cooking temperature range of  $25^\circ\text{C}$  to  $180^\circ\text{C}$ . The accuracy of these temperature readings are dependant on both the sensor accuracy and the electronics accuracy. The electronics accuracy depends on the accuracy of the bridge resistors and ADC, as changes in the temperature would cause changes in the external resistances in the Wheatstone Bridge and in the amplifier in the ADC. The sensor accuracy involves improving the relative accuracy of the sensors against each other. With each SmartChip having two sensors mounted on it, it is crucial that they both take the same readings.

The SmartChip timekeeping is handled by the watchdog timer of the microcontroller. The watchdog timer oscillates at a frequency of 125 kHz at 25°C and interrupts are used to control the sampling interval. The oscillation frequency of the watchdog timer was found to vary with temperature, and so calibration is required to improve the accuracy of these measurements.

This section aims to present the calibration procedure used to maximize the accuracy of the SmartChip readings.

### Electronics Calibration

In a typical case, sensors are thermally isolated from the sensing electronics to achieve more consistent readings, as shown in Figure C2. However, due to the flow-following nature of the SmartChip, the electronics and sensors are all contained in the same package. Maintaining the high accuracy of the sensor in the variable temperature environment requires the stability of the SmartChip electronics over the entire operation range of the temperatures.

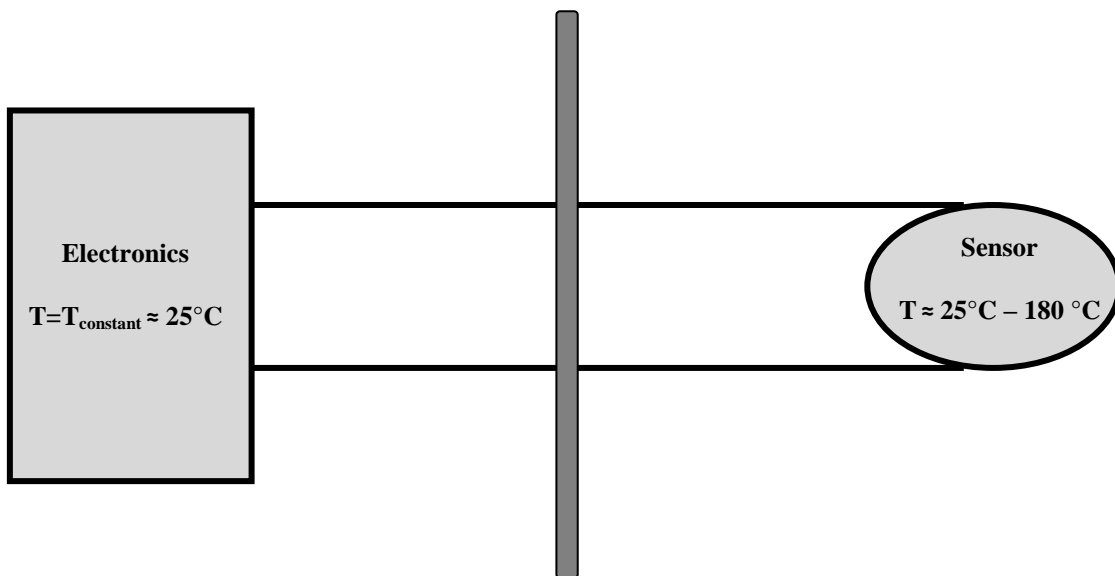
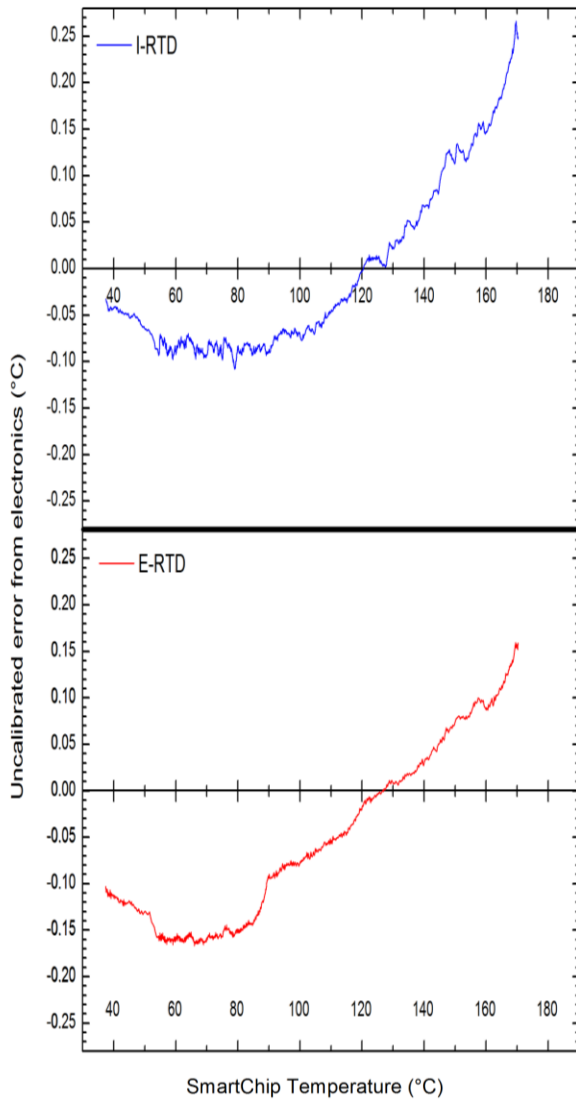


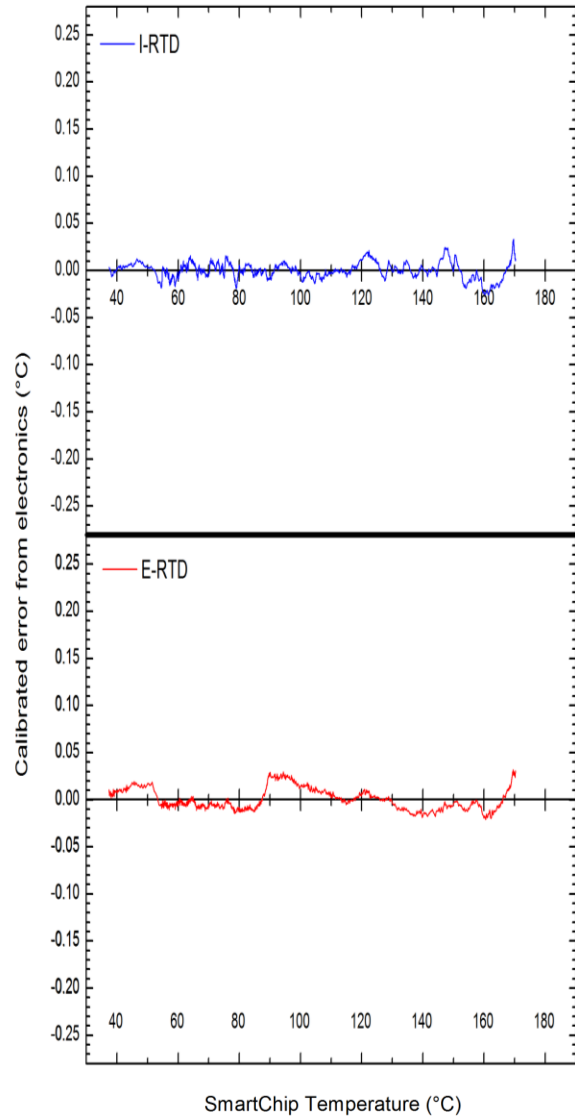
Figure C2: Typical arrangement of sensor and electronics

To determine the actual electronics accuracy, the RTD sensor is replaced with a low TCR  $1572.5\Omega$  resistor to simulate a temperature of exactly  $150.07^{\circ}\text{C}$ . The  $1572.5\Omega$  resistor is kept physically apart from the prototype and thermally insulated at room temperature. The prototype starts taking measurements while it is being heated up to  $180^{\circ}\text{C}$  in 1 hour and then cooled back down to  $25^{\circ}\text{C}$  in 2 hours, while the temperature of the electronics is measured externally. The measurement made by the prototype is then subtracted by  $150.07^{\circ}\text{C}$  to determine the measurement error, and thus the electronics accuracy. Figure C3(a) shows the measurement error from the electronics versus the SmartChip temperature, for each sensor port (I-RTD and E-RTD) on the SmartChip. Though not being presented, the same procedure of SmartChip calibration was adopted for SC002. The uncalibrated electronics error for each of the SmartChip sensor ports was approximately  $\pm 0.3^{\circ}\text{C}$ , and the repetition of the same runs verified that the electronics accuracy was repeatable and could be effectively compensated for by calibration.

A 3<sup>rd</sup> order polynomial calibration function is used to calibrate each sensor port on SC001 for improved SmartChip accuracy, as shown in Figure C3(b). These calibration results could then be applied to subsequent runs – Figure C4 presents the calibrated measurement error from the electronics versus the SmartChip temperature, for each sensor port (I-RTD and E-RTD) on the SC001. Calibration improves the SmartChip accuracy from  $\pm 0.3^{\circ}\text{C}$  to  $\pm 0.1^{\circ}\text{C}$  and the calibration function from one trial holds for the subsequent trials. However due to the electronics operating temperatures, calibration only lasts for approximately ten journeys along the digester and hence recalibration may be required afterwards.



(a)



(b)

**Figure C3: (a) Measuring the uncalibrated electronics error for both sensor ports (I-RTD and E-RTD) on SC001 over the SmartChip temperature range when the SmartChip is heated up to 180°C and then allowed to cool back down to 25°C in 2 hours (b) Calibrated electronics error for both sensor ports (I-RTD and E-RTD) on SC001 over the SmartChip temperature range for the same run.**

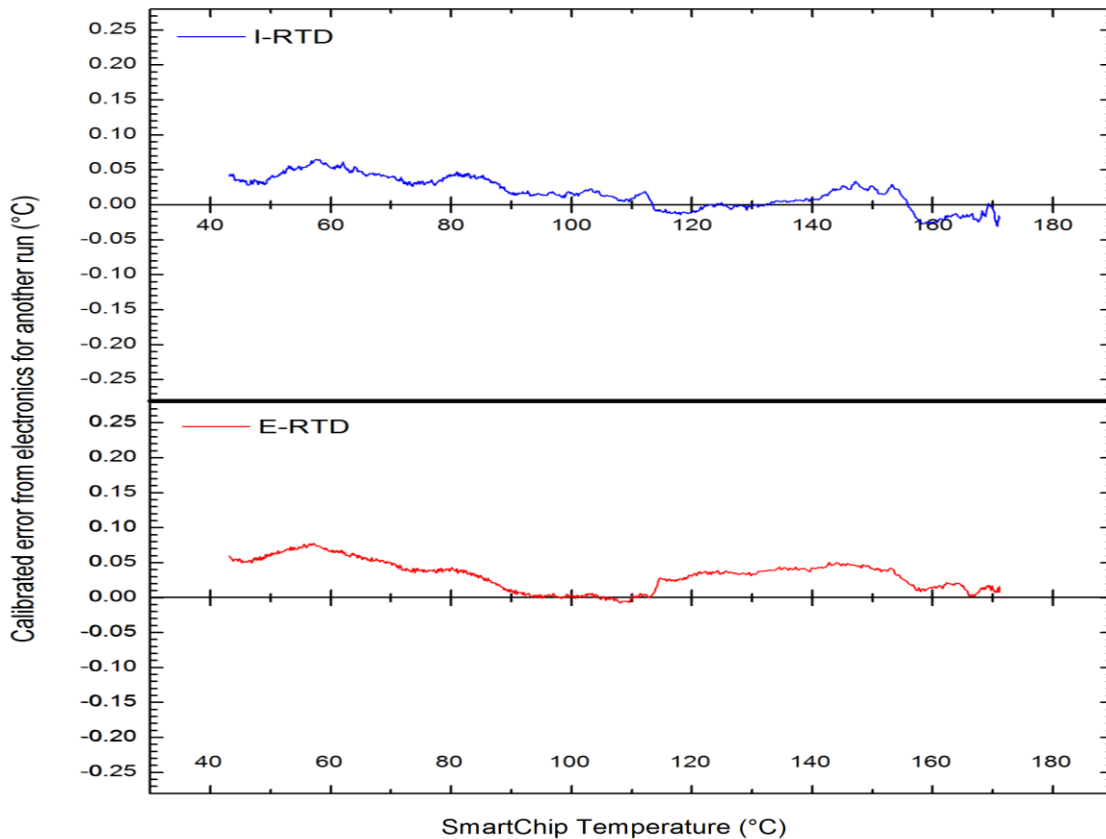


**Figure C4: Calibrated electronics error for both sensor ports (I-RTD and E-RTD) on SC001 over the SmartChip temperature range when the SmartChip is heated up to 180°C and then allowed to cool back down to 25°C in 2 hours – the calibration constant for the previous run are applied to a subsequent run to verify that calibration holds.**

### Sensor Calibration

The temperature sensor chosen for the prototype SmartChip was a thin-film 1000Ω class-A platinum RTD, model F2020 from Omega.ca, with a specified tolerance of  $\pm 0.15 + 0.002T$  °C. Temperature measurements are performed using the Wheatstone Bridge, shown in Figure C1, whose output voltage is proportional to the RTD’s resistance and therefore the temperature. The ADC converts the bridge voltage output to the corresponding digital representation which is then converted to temperature by the Calendar-Van Dusen equation:  $R_T = R_0(1 + AT + BT^2)$  - with the values of the constants  $A$  and  $B$  specified by the product manual. This section focuses on

improving the relative accuracy of the sensors against one another to get them to read the same temperature. The relative accuracy of the sensors is crucial as we are more interested in the temperature variation within the digester. Although it would be ideal to improve the absolute accuracy of the sensors, this process is rather costly and the equipment required are unavailable.

Improved sensor accuracy was established by the calibration of the individual sensors against an oven with a relatively high stability of  $\pm 0.05^{\circ}\text{C}$ . This procedure involved choosing three set points ( $100^{\circ}\text{C}$ ,  $150^{\circ}\text{C}$  and  $170^{\circ}\text{C}$  respectively) at which the oven was heated and then left to settle at the target temperatures for 2 hours. The SmartChip sensors were connected to each other by a heat sink inside the oven so as to provide a better heat conduction than air. The logged temperatures of the SmartChip sensors were then compared against the oven temperatures so as to determine the measurement error. Figure C5 shows the time-temperature data logged by the SmartChip sensor ports during its time inside the oven. The results show that the SmartChip temperature readings vary slightly from the oven temperatures. The logged temperatures for each sensor is converted back into resistance by the Callendar-Van Dusen equation (based on the provided constants) and then a second order polynomial is fit into the actual data so as to readjust the values of the A and B constants in the Callendar–Van Dusen equation for each sensor port – the results of this readjustment are shown in Figure C6.

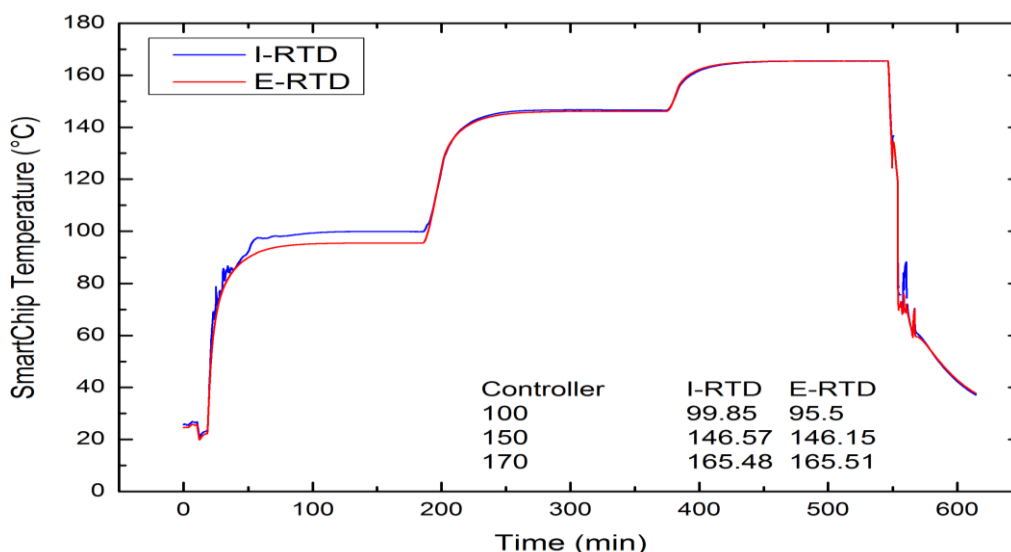
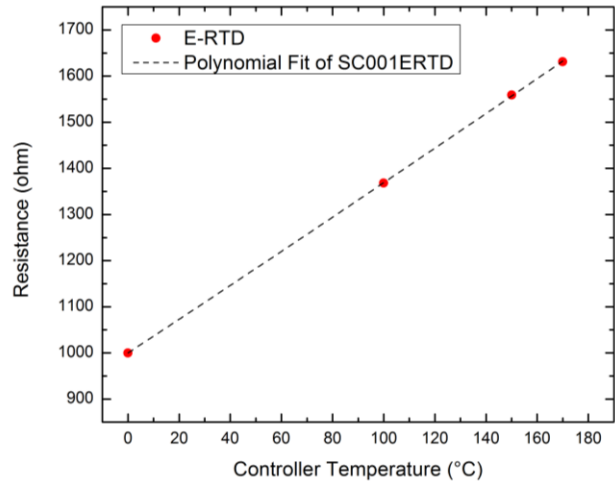
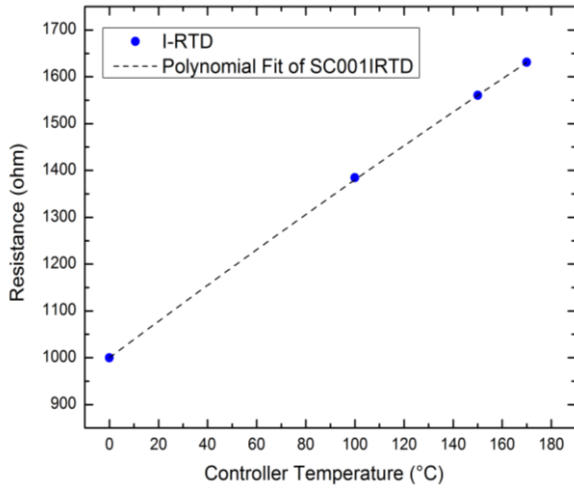


**Figure C5: Time-temperature data logged by the sensor ports (I-RTD and E-RTD) on SC001 when placed in an oven that was heated and allowed to settle at three set points.**



Model	Polynomial		
Equation	$y = \text{Intercept} + B1*x + B2*x^2$		
Weight	No Weighting		
SC001 I-RTD		Value	Standard Error
	Intercept	1000	--
	B1	3.92784	--
	B2	-0.00127	--

Model	Polynomial		
Equation	$y = \text{Intercept} + B1*x + B2*x^2$		
Weight	No Weighting		
SC001 E-RTD		Value	Standard Error
	Intercept	999.8709	2.75891
	B1	3.64462	0.08238
	B2	4.51E-04	4.85E-04

**Figure C6: Fitting the Callendar–Van Dusen to the actual temperature readings taken by each sensor port (I-RTD and E-RTD) on SC001 so as to readjust the A and B constants in this equation.**

Figure C7 presents the sensor calibrated temperature readings for each sensor port (I-RTD and E-RTD) on SC001 based on the readjusted A and B constants in the Callendar–Van Dusen equation when placing the SmartChip in the oven for a second run. These results verify the calibration and improve the relative accuracy of the SmartChips against each other.

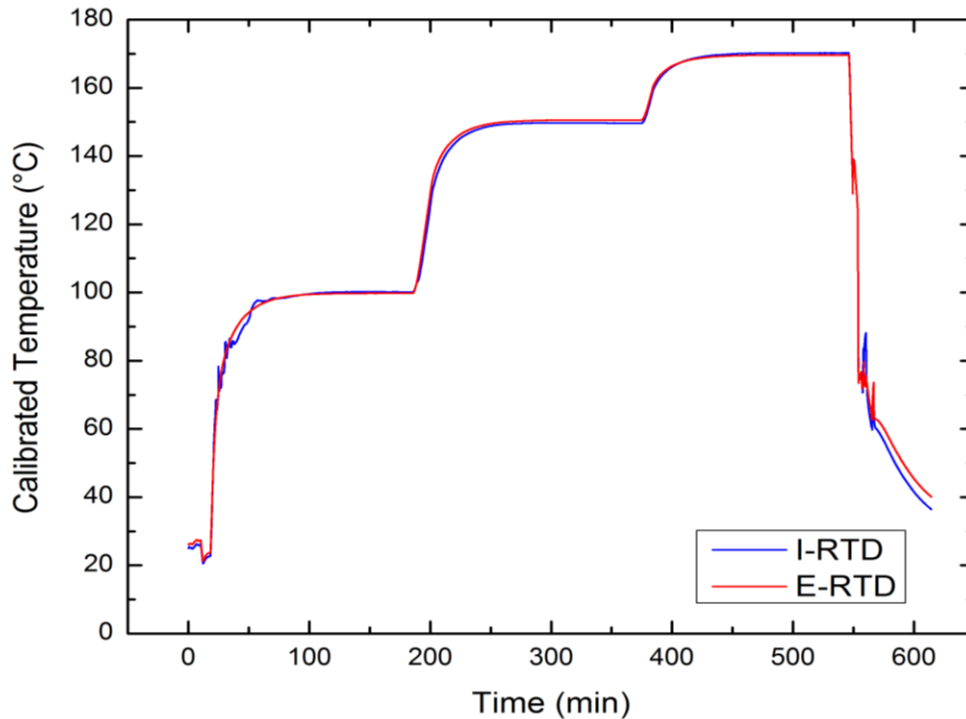


**Figure C7: Calibrated temperature readings for both sensor ports (I-RTD and E-RTD) on SC001 when placed in an oven that was heated and allowed to settle at three set points - the calibration constant for the previous run are applied to a subsequent run to verify that calibration holds.**

### Time Calibration

The oscillation frequency of the watchdog timer was found to vary with temperature such that the temporal error would amount to as much as 20 minutes during a four hour kraft cook. The worst case scenario was seen at about 140°C, where the oscillator slowed by up to 0.5s during the sampling interval.

The accuracy of the time measurements could be improved significantly by calibration. This was done by configuring the SmartChip to generate a digital signal while sampling and then capturing the sampling interval vs. temperature data with an external device while the SmartChip was being cooled from 180°C for 2 hours – as shown in Figure C8. A fourth order polynomial fit was developed to improve the SmartChip timekeeping accuracy, resulting in the temporal error after this calibration to be only 46s during a four hour kraft cook. Figure C9 compares the

uncalibrated and calibrated interval error over the temperature range of 40°C to 180°C – showing a significant improvement in the timekeeping accuracy. After calibration, the temporal error was  $\pm 20$  ms per interval (4 second intervals) – this is also seen in Figure C9.

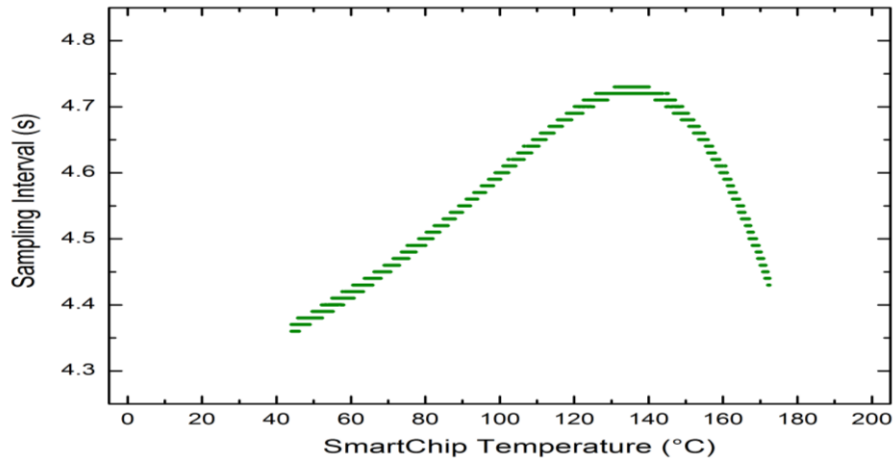


**Figure C8: The variation in the sampling interval with temperature while the SmartChip was cooled down from 180°C.**

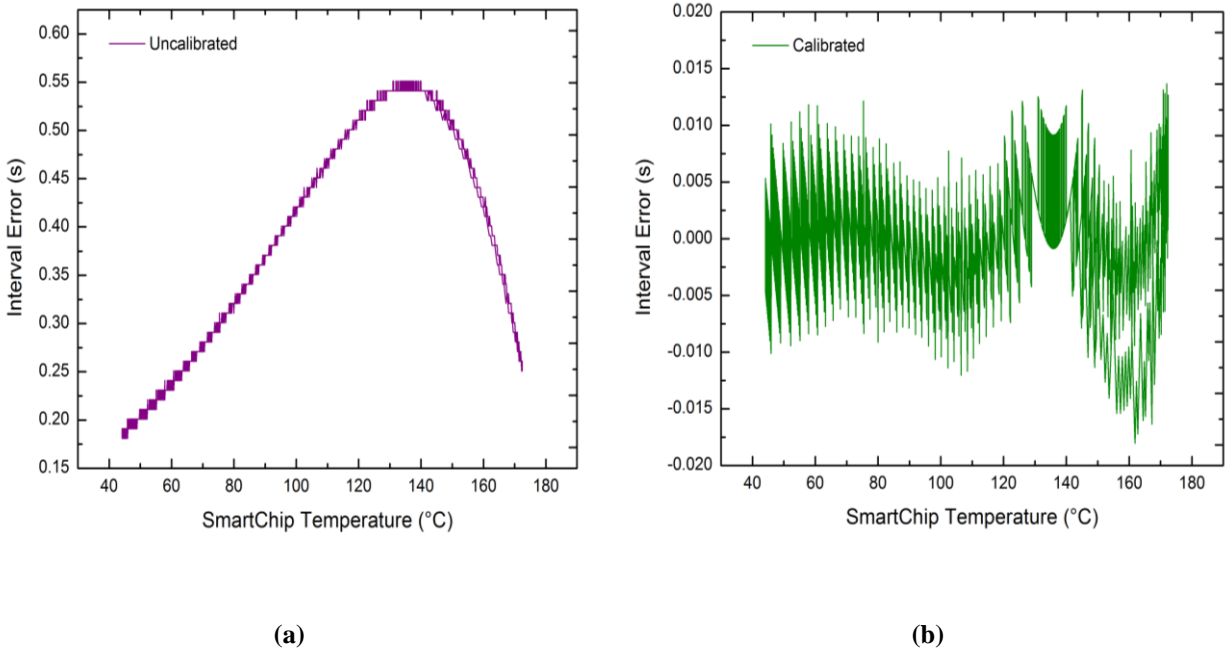


**Figure C9: Comparison of the (a) uncalibrated and (b) calibrated interval error over the SmartChip temperature range of 40°C to 180°C.**